Research Square

Preprints are preliminary reports that have not undergone peer review.
They should not be considered conclusive, used to inform clinical practice,
or referenced by the media as validated information.

Integrative transcriptomic analysis identifies secondary metabolism-related candidate genes associated with salinity tolerance in Medicago sativa

Rugang Yu
Huaibei Normal University
Na Wu
Huaibei Normal University
Lin Yang
Huaibei Normal University
Yanan Gu
Huaibei Normal University
Minyi Liu
Huaibei Normal University
Hanyu Ma
Huaibei Normal University
Xiaona Niu
Huaibei Normal University
Xueling Du
Huaibei Normal University
Guoliang Wang
wangguoliang@126.com

Shandong Academy of Agricultural Sciences

Research Article

Keywords: Salinity stress, Transcriptome analysis, Medicago sativa, Secondary metabolite biosynthesis

Posted Date: November 13th, 2026

DOI: https://doi.org/10.21203/rs.3.rs-11552416/v1

License: This work is licensed under a Creative Commons Attribution 4.0 International License.
Read Full License

Additional Declarations: No competing interests reported.

Integrative transcriptomic analysis identifies secondary metabolism-related candidate genes associated with salinity tolerance in *Medicago sativa*

Rugang Yu[1]

E-mail: yurugang@126.com

Na Wu[1]

E-mail: 3367655993@qq.com

Lin Yang[1]

E-mail: 2627645630@qq.com

Yanan Gu[1]

E-mail: 2767649957@qq.com

Minyi Liu[1]

E-mail: 3425479689@qq.com

Hanyu Ma[1]

E-mail: 582879732@qq.com

Xiaona Niu[1]

E-mail: 1225560952@qq.com

Xueling Du[1]*

E-mail: duxueling1208@126.com

Guoliang Wang[2]*

E-mail: wangguoliang@126.com

[1]*College of Life Sciences, Huaibei Normal University, Huaibei, Anhui 235000, P.R. China;*

2 Institute of Leisure Agriculture, Shandong Academy of Agricultural Sciences, Jinan, Shandong 250100, P.R. China.

[*]**Author for correspondence:**

Dr. Guoliang Wang

Jinan Shandong 250100, P.R. China

E-mail: wangguoliang@126.com.

Xueling Du Assoc. Prof.

Huaibei Anhui 235000, P.R. China

E-mail: duxueling1208@126.com

ABSTRACT

Alfalfa (*Medicago sativa* L.) is one of the most widely cultivated forage legumes worldwide. Soil salinity is a major abiotic stress that adversely affects the alfalfa yield and quality. Secondary metabolites play important roles in plant responses and adaptation to salinity stress. Nevertheless, the key genes involved in secondary metabolite biosynthesis that may contribute to salinity tolerance in alfalfa remain poorly characterized. In this study, time-course transcriptome profiling and comparative transcriptomic analysis was integrated to identify candidate genes associated with secondary metabolic and salinity stress responses in alfalfa. Time-course transcriptome analysis of the salinity-tolerant variety Gibraltar (GIB) identified 521 DEGs associated with secondary metabolite biosynthesis, including 276 genes associated with phenolic compound biosynthesis, 76 related to terpenoid biosynthesis, and 169 related to the biosynthesis of nitrogen-containing compounds. Further integration with a comparative transcriptomic data from GIB and the salinity-sensitive variety LS1405 (LS) identified 87 candidate DEGs for further analysis. Notably, several genes involved in phenolic biosynthesis (*4CLL9*, *ANR*, *UFGT7*, *CSE*, *COMT1*), terpenoid biosynthesis (*HDR*, *SQE1*, *DXS*), and nitrogen-containing compounds biosynthesis (*G8H, STR4, TRI, TAT2, TYDC1, SAMSs,* and *PAO5*) exhibited higher expression levels in roots and/or leaves of GIB than in those of LS under NaCl treatment. These findings suggest that these genes associated with secondary metabolite biosynthesis might contribute to salinity stress adaptation in alfalfa and provide promising targets for future functional studies.

Keywords: Salinity stress; Transcriptome analysis; *Medicago sativa*; Secondary metabolite biosynthesis

1 Introduction

Soil salinization is recognized as one of the major environmental constraints inhibiting plant growth and agricultural productivity (Acharya et al. 2024). Reportedly, saline soils affect more than 1/5 of cultivated land and approximately 1/3 of irrigated farmland globally (Shrivastava and Kumar 2015). Moreover, the continued expansion of salinization soil areas poses an increasing threat to sustainable crop production and food security (Ahmad et al. 2023). Various strategies have been developed to improve the agricultural utilization of saline soil, among which breeding salinity-tolerant crop varieties is considered one of the most promising solutions (Song et al. 2022). Mining genes associated with salinity-tolerant provides valuable genetic resources for improving crop salinity tolerance at molecular level (Ly et al. 2024; Yu et al. 2023). Therefore, elucidating the molecular mechanism underlying plant salinity tolerance is necessary for breeding salinity-tolerant crop varieties.

Plants have evolved various physiological, biochemical, and molecular mechanisms to adapt to salinity stress (Waheed et al. 2024; Yang et al. 2025). Among them, the accumulation of secondary metabolites, including phenolics (e.g. flavonoids and lignins), terpenes (e.g. terpenoids or isoprenoids), and nitrogen-containing compounds (e.g. alkaloids and polyamines), have been extensively implicated in plant responses to environmental stresses (Mahmood et al. 2020; Zhou et al. 2024). For example, overexpression of *CcCAD10* in pigeon pea significantly increased lignin content and antioxidant enzyme activities, thereby

enhancing salinity tolerance (Pan et al. 2025). Similarly, overexpression of the soybean flavonoid biosynthetic gene *GmF3'H* significantly improved the salinity tolerance in transgenic plants (Wu et al. 2026). Carotenoids can scavenge reactive oxygen species (ROS), thereby protecting plants against oxidative damage (Ben-Dor et al. 2005). Furthermore, overexpression of *LcPDS*, *LcZDS*, and *LcCRTISO* in transgenic tobacco enhanced salinity tolerance by regulating carotenoid accumulation (Li et al. 2020). Moreover, overexpressing *MdTyDC* in apple enhanced salinity tolerance by regulating the dopamine accumulation, antioxidant enzyme activities, and ion homeostasis (Wang et al. 2020). Although these studies have demonstrated the importance of secondary metabolism in plant salt stress responses, the potential contributions of secondary metabolite biosynthetic pathways to salt tolerance in alfalfa remain incompletely understood.

Alfalfa (*Medicago sativa* L.) is a widely cultivated perennial forage legumes characterized by wide environmental adaptability, high yield, and high protein content (Yang et al. 2023). China has approximately 170 million ha of saline-alkali land, of which about 50 million ha are considered potentially suitable for agricultural development and utilization (Wang et al. 2025b). Previous study has indicated that alfalfa exhibits moderate salinity tolerance (Sangabriel-Conde et al. 2015). Enhancement of salinity tolerance is therefore a critical focus of alfalfa breeding. Identifying the genes and regulatory mechanisms underlying salinity stress adaptation is essential for developing salinity-tolerant alfalfa varieties. Recent advances in RNA-sequencing (RNA-Seq) have facilitated the identification of

numerous salinity-responsive genes in alfalfa (Yang et al. 2024; Zhu et al. 2026). For example, Yang et al. (2024) identified several genes associated with ion homeostasis and osmotic stress responses, including *HPCA1-LRR*, *PP2C60*, *PP2C71*, *CRK1*, *APX3*, *HXK2*, *BAG6*, and *ARF1*, as potential contributors to salinity adaptation in alfalfa. Similarly, Zhu et al. (2026) compared the transcriptional responses of the salinity-tolerant alfalfa variety ZangMu 1 and the salinity-sensitive variety ZangMu 2 and found that genes associated with flavonoid biosynthesis may play important roles in salinity tolerance. Despite these advances, the molecular mechanisms underlying salinity tolerance in alfalfa, particularly those associated with secondary metabolism, remain elusive.

We hypothesized that salinity tolerance in alfalfa may be associated with the differential regulation of genes involved in secondary metabolite biosynthesis under salinity stress. To investigate this hypothesis, we performed time-course transcriptomic analyses of roots and leaves from the salinity-tolerant alfalfa variety Gibraltar (GIB) at different time points following NaCl treatment. We further integrated these data with an independent comparative transcriptomic dataset from the salt-tolerant variety GIB and the salt-sensitive variety LS1405 (LS). The objectives of this study were to characterize temporal transcriptional changes in roots and leaves following salinity treatment and to identify candidate genes involved in secondary metabolite biosynthesis that may be associated with salinity tolerance in alfalfa. The findings presented here will help to understand the molecular mechanism of salinity tolerance of GIB variety and provide potential targets for

130 future breeding efforts aimed at improving salinity tolerance in alfalfa.

131

2 Materials and methods

2.1 Plant materials and salinity treatments

The salinity-tolerant alfalfa variety GIB was used in this study (Yu et al. 2021). Seeds were obtained commercially from the Beijing Best Grass Industry Co., Ltd. Surface-sterilized seeds were sown in containers (12 cm × 12 cm) filled with washed sand under a 16/8h light/dark cycle for two weeks. Uniform seedlings were then cultivated in black plastic box for two weeks, with six plants per box. Each box contained 800 mL of Hoagland nutrient solution (pH 5.8).

For the salinity stress experiment, four-week-old seedlings were exposed to 200 mM NaCl. Root and leaf samples were collected at 0 (control), 24 and 72 h, with three biological replicates per sampling time point and tissue type. Each biological replicate consisted of six individual plants. All harvested samples were immediately frozen in liquid nitrogen and stored at-80°C for RNA-seq and Reverse-transcription quantitative PCR (RT-qPCR) validation.

2.2 cDNA library preparation and RNA sequencing

Total RNA was extracted from root and leaf samples of GIB collected at three different time points after NaCl stress using QIAzol Lysis Reagent (Qiagen) following the supplier's instructions. RNA concentration and purity were evaluated using a Nanodrop 2000. A total of 18 cDNA libraries were constructed, comprising nine root libraries (R_0_1, R_0_2, R_0_3, R_{24}_1, R_{24}_2, R_{24}_3, R_{72}_1, R_{72}_2, and R_{72}_3) and nine leaf libraries (L_0_1, L_0_2, L_0_3, L_{24}_1, L_{24}_2, L_{24}_3, L_{72}_1, L_{72}_2 and L_{72}_3). Each library was prepared from 10 ng of total RNA using the SMART-Seq v4 Ultra Low

Input RNA Kit (Clontech, San Diego, CA, USA). Paired-end sequencing was performed on the DNBSEQ-T7 platform using the DNBSEQ-T7RS Reagent Kit (FCL PE150, version 3.0). Library preparation and sequencing were conducted by Shanghai Majorbio Bio-pharm Technology Co., Ltd. (Shanghai, China). Raw sequencing reads were processed using fastp (https://github.com/OpenGene/fastp) with default parameters to remove low-quality reads and adapter sequences. The resulting high-quality clean reads were aligned to the alfalfa reference genome using HiSat2 (http://ccb.jhu.edu/software/hisat2/index.shtml). Transcript assembly was subsequently performed for each sample using StringTie (http://ccb.jhu.edu/software/stringtie/).

2.3 Identification and functional enrichment analysis of differentially expressed genes (DEGs)

Gene expression levels were quantified as transcripts per million reads (TPM), and gene-level expected read counts were generated using RSEM (http://deweylab.github.io/RSEM/). Read counts were adopted to determine the differential expression analysis by the DESeq 2 (http://bioconductor.org/packages/stats/bioc/DESeq2/) based on the negative binomial distribution. The false discovery rate (FDR) was used to correct the statistical significance of multiple tests. Genes satisfying the criteria of $|\log_2$ fold change$|> 1$ and FDR< 0.05 were considered differentially expressed.

Functional annotation and enrichment analyses of DEGs was performed using Gene Ontology (GO) and Kyoto Encyclopedia of Genes and Genomes (KEGG). GO terms

and KEGG pathways with Bonferroni-corrected *P*-value≤ 0.05 were considered significantly enriched, using all genes included in the transcriptome analysis as the reference background.

2.4 Integration of time-course and comparative transcriptome datasets

The time-course transcriptome dataset was used to characterize gene expression changes following exposure to 200 mM NaCl, using the 0 h samples as the datum. Because time-matched untreated controls were not available at 24 and 72 h, the observed temporal changes could not be attributed exclusively to salinity stress. Therefore, an independent comparative transcriptome dataset containing both untreated and salinity-treated samples was incorporated to provide additional evidence for prioritizing candidate genes potentially associated with salinity tolerance.

The comparative transcriptome dataset was downloaded from the Genome Sequence Archive at Beijing Institute of Genomics (China National Center for Bioinformation) (https://ngdc.cncb.ac.cn/gsa/search?searchTerm=CRA012389) (Yu et al. 2025). In the published study, two weeks after sowing, seedlings of the salinity-tolerant variety GIB and the salinity-sensitive variety LS1405 (LS) were subjected to either 0 or 200 mM NaCl treatment. Salinity treatment lasts for two weeks, and root and leaf samples were harvested for transcriptome sequencing (Yu et al. 2025). Gene expression values (Fragments Per Kilobase of transcript per Million mapped fragments, FPKM) from roots and leaves under 0 and 200 mM NaCl treatments were extracted for subsequent analyses.

Candidate genes were identified through a stepwise screening strategy. Firstly,

DEGs annotated as being involved in secondary metabolite biosynthesis were extracted from the time-course transcriptome dataset. Among these genes, those exhibiting significant upregulation in at least two pairwise comparisons within the same tissue were retained for further analysis. Secondly, the expression profiles of these selected genes were examined using the comparative transcriptome dataset from GIB and LS to identify potential candidate genes associated with salinity tolerance and secondary metabolite biosynthesis in alfalfa.

2.5 RT-qPCR validation

Total RNA was extracted from GIB root and leaf tissues using TRIzol reagent (Invitrogen, USA). First-strand cDNA synthesis was performed using the Prime Script® RT reagent Kit (Takara). RT-qPCR was carried out on an ABI7300 Real-Time PCR System (Applied Biosystems, Foster City, CA, USA) using SYBR Premix Ex Taq Kit (Takara) according to the manual. The *MsActin* gene served as the internal reference for normalization. Primer sequences used in this study are listed in Table S1. Relative expression level of each gene was calculated using the $2^{-\Delta\Delta CT}$ method.

2.6 Statistical analysis

Statistical analyses were conducted using SPSS 25.0. Data are expressed as means ± SD based on three independent replicates. Differences in gene relative expression levels were assessed using one-way analysis of variance (ANOVA) and Duncan test at $P < 0.05$.

3 Results

3.1 Sequencing of 18 roots and leaves cDNA libraries in alfalfa

To identify the functional genes involved in salinity stress tolerance in alfalfa, 18 cDNA libraries from the roots (R_{0_1}, R_{0_2}, R_{0_3}, R_{24_1}, R_{24_2}, R_{24_3}, R_{72_1}, R_{72_2}, R_{72_3}) and leaves (L_{0_1}, L_{0_2}, L_{0_3}, L_{24_1}, L_{24_2}, L_{24_3}, L_{72_1}, L_{72_2} and L_{72_3}) at 0, 24 and 72 h after NaCl treatment were constructed and sequenced. Approximately 44.2-57.7 Mb raw reads were produced in each cDNA library. After adapter trimming and removal of low-quality sequences and reads with ambiguous nucleotides, 43.9-57.2 Mb clean reads were successfully obtained in each cDNA library, with more than 94.5% Q30 bases and 41.51% GC content. Further analysis revealed that over 44.03 Mb clean reads (89.83 %) were total mapped to the alfalfa reference genome in each library (Table S2). These results suggested that the sequencing data were of sufficient quality for subsequent transcriptomic analyses.

3.2 Identification of differentially expressed genes (DEGs)

DEGs in pairwise comparison of roots (R_{24}/R_0, R_{72}/R_0, R_{72}/R_{24}) or leaves (L_{24}/L_0, L_{72}/L_0, L_{72}/L_{24}) of GIB at 0, 24, and 72 h after salinity stress were filtered using thresholds of $|\log_2$ fold change$|> 1$ and FDR< 0.05 (Table S3). Here, 16,457 DEGs were identified in the R_{24}/R_0, comprising 8341 up-regulated and 8116 down-regulated genes. The R_{72}/R_0 identified 14,527 DEGs, including 6299 up-regulated and 8228 down-regulated genes (Figure 1A). In addition, 18,210 DEGs were identified in L_{24}/L_0, among which 8075 were upregulated and 10,135 were downregulated. Meanwhile, 12,887 DEGs were identified in L_{72}/L_0, consisting of

5612 upregulated and 7275 downregulated genes (Figure 1A). Moreover, 379 shared DEGs were up-regulated in R_{24}/R_0, R_{72}/R_0, L_{24}/L_0, L_{72}/L_0 (Figure 1B), while 667 shared DEGs down-regulated (Figure 1C).

3.3 GO analysis of DEGs

We performed GO enrichment analysis for determining major functions of DEGs, a total of 686, 474, 724, 1001, 676 and 773 enriched GO terms (P_{adj}-value < 0.05) acquired in R_{24}/R_0, R_{72}/R_0, R_{72}/R_{24}, L_{24}/L_0, L_{72}/L_0, L_{72}/L_{24}, respectively. These terms were distributed among the three GO categories: biological process, cellular component, and molecular function (Table S4). The top 20 enriched GO terms for DEGs in each comparison are shown in Figure 2. Furthermore, 236 and 279 GO terms were common enriched in roots (R_{24}/R_0, R_{72}/R_0, R_{72}/R_{24}) and leaves (L_{24}/L_0, L_{72}/L_0, L_{72}/L_{24}), respectively (Table S5). Within root tissues, enriched biological processes were mainly associated with secondary metabolic process (GO:0019748), small molecule metabolism (GO:0044281) and phenylpropanoid metabolism (GO:0009698); Cellular component enrichment was predominantly related to the extracellular region (GO:0005576), membrane structures (GO:0016020), and plasma membrane (GO:0005886). Molecular functions were mainly represented by oxidoreductase activity (GO:0016491), heme binding (GO:0020037), and tetrapyrrole binding (GO:0046906) (Table S5). In leaf tissues, significantly enriched biological processes included small-molecule metabolism (GO:0044281), carboxylic acid metabolism (GO:0019752), and organic substance biosynthesis (GO:1901576). Meanwhile, plastids (GO:0009536), chloroplasts (GO:0009507), and plastid stroma

(GO:0009532), were highly represented within the cellular component category. Molecular function analysis indicated significant enrichment of oxidoreductase activity (GO:0016491), catalytic activity (GO:0003824), and phosphoric ester hydrolase activity (GO:0042578) (Table S5).

3.4 KEGG metabolic pathway analysis of DEGs

To gain further insight into the biological pathways affected by salinity stress, KEGG enrichment analysis was performed for all DEGs. In total, 133 pathways were identified across all comparisons and could be assigned to five functional categories, including metabolism, genetic information processing, environmental information processing, cellular processes, and organismal systems (Table S6). Among them, significant enrichment ($P_{adj} < 0.05$) was observed for 29 pathways in R_{24}/R_0, 15 pathways in R_{72}/R_0, 33 pathways in R_{72}/R_{24}, 49 pathways in L_{24}/L_0, 22 pathways in L_{72}/L_0, and 29 pathways in L_{72}/L_{24} (Table S6). For DEGs in roots, phenylpropanoid biosynthesis (ko00940) represented the most consistently enriched pathway in R_{24}/R_0, R_{72}/R_0 and R_{72}/R_{24} (Table 1 and Figure 3A-C). Additional highly enriched pathways included nitrogen metabolism (ko00910) and biosynthesis of various plant secondary metabolites (ko00999) in R_{24}/R_0 (Table 1 and Figure 3A), ribosome (ko03010) and circadian rhythm–plant (ko04712) in R_{72}/R_0 (Figure 3B), as well as isoflavonoid biosynthesis (ko00943) and biosynthesis of various plant secondary metabolites (ko00999) in R_{72}/R_{24} (Table 1 and Figure 3C). For DEGs in leaves, porphyrin metabolism (ko00860), isoquinoline alkaloid biosynthesis (ko00950), and α-linolenic acid metabolism (ko00592) were among the most

284 significantly enriched pathways in L_{24}/L_0 (Figure 3D). Ribosome (ko03010), MAPK
285 signaling pathway–plant (ko04016), and riboflavin metabolism (ko00740) were
286 dominant in L_{72}/L_0 (Figure 3E), whereas ribosome (ko03010), porphyrin metabolism
287 (ko00860), and selenocompound metabolism (ko00450) were most significantly
288 enriched in L_{72}/L_{24} (Figure 3F). Furthermore, 12 pathways (e.g. phenylpropanoid
289 biosynthesis, biosynthesis of various plant secondary metabolites, tropane, piperidine
290 and pyridine alkaloid biosynthesis) shared significantly enriched in R_{24}/R_0, R_{72}/R_0
291 and R_{72}/R_{24}, and 10 pathways (e.g. phenylalanine metabolism, Carbon fixation in
292 photosynthetic organisms, and carotenoid biosynthesis) shared significantly enriched in
293 L_{24}/L_0, L_{72}/L_0 and L_{72}/L_{24} were obtained (Table S6).

294 ***3.5 DEGs associated with the biosynthetic pathways of phenolic compounds***

295 In total, 276 DEGs encoding enzymes related to phenolic compounds biosynthesis
296 were identified (Table S7). These genes were assigned to key steps of the flavonoid,
297 anthocyanin and lignin biosynthetic, including phenylalanine ammonia lyase (PAL),
298 cinnamic acid 4-hydroxylase (C4H), 4-coumarinyl-CoA ligase (4CL), chalcone
299 synthase (CHS), chalcone isomerase (CHI), isoflavone synthase (IFS), flavone
300 synthase (FNS), flavanone 3-hydroxylase (F3H), flavonol synthetase (FLS),
301 flavonoid 3′-hydroxylase (F3′H), dihydroflavonol reductase (DFR), anthocyanin
302 synthase (ANS), anthocyanidin reductase (ANR), UDP-glucose flavonoid
303 3-O-glucosyltransferase (UFGT), hydroxycinnamoyl CoA: shikimate
304 hydroxycinnamoyl transferase (HCT), coumaroyl shikimate 3′-hydroxylase (C3′H),
305 caffeoyl shikimate esterase (CSE), caffeate/5-hydroxy-coniferaldehyde

306 3/5-O-methyltransferase (COMT), ferulate/coniferaldehyde 5-hydroxylase (F5H),
307 caffeoyl-CoA O-methyltransferase (CCoAOMT), cinnamoyl CoA reductase (CCR),
308 cinnamyl alcohol dehydrogenase(CAD) (Table S7). Among them, 4*CLL9*
309 (MS.gene022445), *COMT1* (MS.gene024383), *CCR1* (MS.gene64416), *CAD1*
310 (MS.gene002258), *CSE* (MS.gene75172/76310), *CCoAOMT2*
311 (MS.gene56793/99216), and *UFGT7*
312 (MS.gene049907/00212/011829/28593/67515/90522/99188) genes were upregulated
313 in at least two pairwise comparisons of R_{24}/R_0, R_{72}/R_0 and R_{72}/R_{24} (Figure 4).
314 Furthermore, 4*CLL9* (MS.gene004713), *ANR* (MS.gene01410), *HCT*
315 (MS.gene054539), *CAD2* (MS.gene065692), *CCoAOMT3* (MS.gene030303),
316 *UFGT7* (MS.gene036571/21268), *COMT1* (MS.gene020301/065217/069457),
317 *CCoAOMT5* (MS.gene011778/041940/90469), *CCR1*
318 (MS.gene64416/034132/052599), and *CAD1* (MS.gene002257/01231/02214) genes
319 were upregulated in at least two pairwise comparisons among L_{24}/L_0, L_{72}/L_0, and
320 L_{72}/L_{24} (Figure 4).

321 ***3.6 DEGs involved in the biosynthetic pathways of terpene compounds***

322 Terpenes (terpenoids or isoprenoids) were synthesized by two independent pathways:
323 the plastid methylerythritol phosphate (MEP) pathway and the cytosolic mevalonate
324 (MVA) pathway. In this study, a total of 76 DEGs encoding enzymes involved in
325 terpenoid compounds biosynthesis were identified, such as β-amyrin synthase (BAS),
326 1-deoxy-D-xylulose-5-phosphate synthase (DXS), geranylgeranyl diphosphate
327 synthase (GGDS), hydroxy-2-methyl-2-(E)-butenyl 4-diphosphate reductase (HDR),

3-hydroxy-3-methyl-glutaryl coenzyme A reductase (HMGR), 3-hydroxy-3-methyl-glutaryl coenzyme A synthase (HMGS), isopentenyl diphosphate isomerase (IDI), mevalonate kinase (MVK), squalene monooxygenase (SMO),squalene synthase (SQS), and squalene epoxidase (SQE) (Table S8). Among them, *MVK* (MS.gene072461), *IDI1* (MS.gene033475), *IDI2* (MS.gene51160), *HDR* (MS.gene40678), *SQS2* (MS.gene50719), *SMO* (MS.gene80337), *DXS* (MS.gene96182), *HMGS* (MS.gene015517/025733), *SQE1* (MS.gene24516/40110) and *BAS* (MS.gene034307/019797) genes were upregulated in at least two pairwise comparisons among R_{24}/R_0, R_{72}/R_0 and R_{72}/R_{24} (Figure 5). In addition, *IDI1* (MS.gene033475), *IDI2* (MS.gene51160), *HDR* (MS.gene40678), *SQE1* (MS.gene001138), *SMO1* (MS.gene32851), *HMGS* (MS.gene015517), *GGDS* (MS.gene87404/28490) and *DXS* (MS.gene014804/060356) genes were upregulated in at least two pairwise comparisons among L_{24}/L_0, L_{72}/L_0, and L_{72}/L_{24} (Figure 5).

3.7 DEGs associated with the biosynthetic pathways of nitrogen-containing compounds

In total, 169 DEGs encoding enzymes related to nitrogen-containing compounds biosynthesis were identified. These enzymes included arginine decarboxylase (ADC), geraniol 8-hydroxylase (G8H), ornithine decarboxylase (ODC), polyamine oxidase (PAO), S-adenosylmethionine synthase (SAMS), S-adenosylmethionine decarboxylase (SAMDC), spermine synthase (SPMS), spermidine synthase (SPDS), strictosidine synthase (STR), tyrosine aminotransferase (TAT), tropinone reductase 1 (TRI) and tyrosine decarboxylase (TYDC) (Table S9). Of them, *ADC*

(MS.gene23355), *TRI* (MS.gene63490), *PAO2* (MS.gene059924), *SAMS3* (MS.gene47449), *SAMS* (MS.gene050426/26796), *ODC* (MS.gene014375/52797) and *G8H* (MS.gene005805/006454, MS.gene037889/066931) genes were upregulated in at least two pairwise comparisons among R_{24}/R_0, R_{72}/R_0, and R_{72}/R_{24} (Figure 6). Moreover, 24 DEGs were upregulated in at least two pairwise comparisons among L_{24}/L_0, L_{72}/L_0, and L_{72}/L_{24}, including *SAMS* (MS.gene050426), *SAMS3* (MS.gene007396/22399), *SAMDC* (MS.gene022054), *PAO5* (MS.gene026071/21960/85388), *STR4* (MS.gene64464), *TAT2* (MS.gene032280, MS.gene34230/36049), *TRI* (MS.gene30551/41122/46110), *TYDC1* (MS.gene003256/02053/03160), *STR10* (MS.gene038383/062331/39129) and *G8H* (MS.gene005807/006077/010726/60535) (Figure 6).

3.8 Correlation analysis of 87 up-regulated genes mentioned above in existing comparative transcriptome data

Based on the above data, 87 genes upregulated in at least two pairwise comparisons in roots and/or leaves of GIB were used to further identify their expression changes in existing comparative transcriptome data in GIB and LS under salinity stress (Table S10). The mRNA sequence information of 87 genes from comparative transcriptome data were obtained based on the Basic Local Alignment Search Tool (BLAST), and then the expression data (FPKM value) of 87 genes were picked out (Table S10). Among them, the expression trends of 56 genes in GIB roots and/or leaves under salinity stress were well consistent with the results of comparative transcriptome sequencing data (Table S11). Notably, the expression of 33 genes, such as *4CLL9*

(MS.gene022445), *SQE1* (MS.gene24516) and *ADC* (MS.gene23355) showed upward trend by salinity treatment in roots and/or leaves in GIB, while in LS, they showed downward trend (Table S11). Moreover, under salinity stress condition, *4CLL9* (MS.gene022445), *ANR* (MS.gene01410) and *UFGT7* (MS.gene049907), *CSE* (MS.gene76310), *COMT1* (MS.gene065217), *HDR* (MS.gene40678), *SQE1* (MS.gene24516), *DXS* (MS.gene96182), *G8H* (MS.gene066931/010726/037889), *STR4* (MS.gene64464), *TRI* (MS.gene46110), *TAT2* (MS.gene032280/34230/36049), *TYDC1* (MS.gene003256/03160), *SAMS* (MS.gene050426/26796), *SAMS3* (MS.gene22399/007396/47449), and *PAO5* (MS.gene026071/21960/85388), showed higher expression in roots and/or leaves of GIB than in LS (Table S11).

3.9 RT-qPCR validation of RNA-seq data

To validate the RNA-Seq results, ten genes (*BAS* MS.gene034307, *CCR1* MS.gene034244, *G8H* MS.gene20003, *IDI1* MS.gene033475, *4CL7* MS.gene09104, *CAD2* MS.gene065692, *FLS1* MS.gene018954, *COMT1* MS.gene024383, *CCR1X2* MS.gene64416, *SAMS* MS.gene050426) related to secondary metabolism biosynthesis were selected for RT-qPCR analysis (Table S1). Nine genes exhibited expression profiles that were consistent with the RNA-seq data (Figure 7), whereas *SAMS* (MS.gene050426) showed a divergent expression pattern between the two methods (Figure 7). These discrepancies between RT-qPCR and RNA-Seq may be attributable to differences in sensitivity between the two methods and need to be further studied. Linear regression analysis showed a correlation coefficient of 0.849 between RT-qPCR and RNA-seq data, confirming the reliability of the RNA-Seq data (Figure

394 8).

4 Discussion

4.1 Transcriptional responses of roots and leaves to salinity stress in GIB

RNA sequencing has become a powerful approach for dissecting regulatory networks and identifying genes involved in key biological processes. In alfalfa, transcriptome-based studies have successfully revealed numerous molecular pathways associated with salinity adaptation (An et al. 2022; Yin et al. 2023). Nevertheless, a systematic investigation focusing specifically on secondary metabolic biosynthesis-related genes of alfalfa in response to salinity stress has not been explored. Here, a total of 16,457, 14,527, 16,967, 18,210, 12,887 and 14,838 genes were identified significant differential expression in R_{24}/R_0, R_{72}/R_0, R_{72}/R_{24}, L_{24}/L_0, L_{72}/L_0 and L_{72}/L_{24}, respectively (Figure 1A). Functional enrichment analysis further revealed 69 significantly enriched KEGG pathways (Table S6), highlighting the complexity of molecular responses triggered by salinity. Of them, 12 and 10 pathways showed significant enrichment of DEGs in roots and/or leaves in all comparisons, respectively (Table S1). Several of these pathways, including phenylpropanoid biosynthesis (ko00940), biosynthesis of various plant secondary metabolites (ko00999), tropane, piperidine and pyridine alkaloid biosynthesis (ko00960), phenylalanine metabolism (ko00360), carotenoid biosynthesis (ko00906), isoflavonoid biosynthesis (ko00943) and flavonoid biosynthesis (ko00941), have previously been linked to salinity stress adaptation (Jia et al. 2025; Liu et al. 2025; Zhu et al. 2021). These results suggested that the DEGs involved in these secondary

metabolism pathways contributing to salinity stress adaptation in alfalfa salinity-tolerant variety GIB.

4.2 DEGs involved in secondary metabolism biosynthetic pathway

4.2.1 DEGs involved in metabolic pathway of phenolic compounds

Phenolic compounds, such as flavonoids and lignin, have been recognized as a major contributor to the plant adaptation under salinity environment (Mahmood et al. 2020; Zhou et al. 2024). Flavonoids are divided into six subcategories, including flavones, flavonols, isoflavones, flavanones, flavanols and anthocyanidins (Białek et al. 2025). The biosynthesis of these compounds is mediated by a series of enzymes such as ANS, ANR, C4H, 4CL, CHS, CHI, DFR, FNS, F3H, FLS, IFS, LAR, PAL and UFGT (He et al. 2023). Previous studies have demonstrated that activation of flavonoid accumulation can enhance plant tolerance to salinity (Ni et al. 2025; Wu et al. 2026). For example, *GmbZIP131* gene has been shown to improve soybean salinity tolerance by promoting flavonoid biosynthesis through a signaling cascade reaction (Ni et al. 2025). In this study, 171 DEGs encoding nine enzyme families (PAL, 4CL, CHS, CHI, FLS, F3′H, DFR, ANR, UFGT) involved in flavonoids biosynthesis were identified in the salinity-tolerant variety GIB at three time points after salinity stress (Table S7). Among them, 12 genes exhibited significant upregulation in at least two pairwise comparisons in roots and/or leaves (Table S10 and Figure 4). Importantly, the expression of 6 out of 12 DEGs including *4CLL9* (MS.gene022445), *ANR* (MS.gene01410) and *UFGT7* (MS.gene00212, MS.gene28593, MS.gene049907,

MS.gene21268) showed upward trend by salinity treatment in roots and/or leaves in GIB, while in LS, they showed downward trend (Table S11). Of them, under salinity stress condition, *4CLL9* (MS.gene022445), *ANR* (MS.gene01410) and *UFGT7* (MS.gene049907) showed higher expression in roots and/or leaves of GIB than in LS (Table S11). In plants, the 4CL enzyme occupies a central position in phenylpropanoid metabolism and participates in the synthesis of both lignin and flavonoid compounds (Lavhale et al. 2018). *St4CL5* promoted the accumulation of lignin and flavonoids, and improved the ability of scavenging ROS, thus improving the ability of potato to resist abiotic stress (Nie et al. 2023). Likewise, ANR functions as a key catalytic enzyme in the production of flavan-3-ols and proanthocyanidins. Overexpression of *RrANR* gene from *Rosa rugosa* significantly increased abiotic stress tolerance in tobacco by enhancing ROS scavenging and influencing ABA-dependent signaling pathways (Luo et al. 2016). UFGT is known to belong to the key enzyme involved in anthocyanin synthesis, and transgenic *Arabidopsis thaliana* plants overexpressing *CrUGT87A1* gene from *Carex rigescens* exhibited enhanced the resistance to salinity by elevated flavonoid content (Zhang et al. 2021). These findings suggested that *4CLL9*, *ANR* and *UFGT7* genes might be the major factors contributing to salinity stress adaptation in alfalfa salinity-tolerant variety GIB.

Lignin polymer is mainly comprised of three major monomers (sinapylalcohol, S unit; coniferylalcohol, G unit and p-coumarylalcohol, H unit) that are synthesized via the phenylpropanoid pathway (Liu et al. 2018). Increasing evidence have indicated that the key enzymes of lignin biosynthesis play an active role in regulating the plant

adaptation to abiotic stress, including HCT (Ma et al. 2025), COMT (Chang et al. 2021; Ge et al. 2023), CAD (Wu et al. 2023), CSE (Kim et al. 2023), CCoAMT (Zhao et al. 2021), CCR (Zhan et al. 2025). In this study, totally 105 DEGs encoding seven enzyme families (HCT, CSE, COMT, CCR, CAD, F5H, CCoAOMT) involved in lignin biosynthesis were identified in GIB at three different time points after salinity stress (Table S7). Of them, 21 genes were upregulated in at least two pairwise comparisons in roots and/or leaves of GIB variety (Table S10 and Figure 4). Importantly, 14 of these genes, including *HCT* (MS.gene054539), *CSE* (MS.gene76310), *CAD2* (MS.gene065692), CCR1 (MS.gene64416/034132), *COMT1* (MS.gene024383/065217/069457), CCoAOMT2 (MS.gene56793/99216), CCoAOMT3 (MS.gene030303) and *CCoAOMT5* (MS.gene011778/041940/90469), showed increased transcript expression in roots and/or leaves in GIB following salinity treatment but showed the opposite trend in LS (Table S11). Among them, *CSE* (MS.gene76310) and *COMT1* (MS.gene065217) showed higher expression in roots and/or leaves of salinity-tolerant variety GIB than in salinity-sensitive variety LS under salinity stress condition (Table S11). Given the established functions of lignin biosynthesis in strengthening cell wall integrity and improving environmental adaptability, implying that *CSE* and *COMT1* genes may contribute to salinity stress adaptation in alfalfa salinity-tolerant variety GIB.

4.2.2 DEGs involved in the biosynthetic pathways of terpene compounds

Terpenoids otherwise known as isoprenoids are often divided into monoterpenes, sesquiterpenes, diterpenes and triterpenes, etc. according to the isoprene structure.

Numerous studies have demonstrated that these compounds play important roles in plant adaptation to abiotic stress (Wen et al. 2024; Zhang et al. 2023). In this study, 76 DEGs encoding 16 enzyme families (e.g. HMGS, HMGR, MVK) associated with terpenoids biosynthesis were identified in GIB under salinity stress (Table S8). Among these genes, 19 showed significant upregulation in at least two pairwise comparisons in roots and/or leaves of the salinity- tolerant variety GIB under salinity stress (Table S10 and Figure 5). Notably, nine genes, including *HMGS* (MS.gene025733), *MVK* (MS.gene072461), *HDR* (MS.gene40678), *SQE1* (MS.gene24516), *BAS* (MS.gene034307), *SMO1* (MS.gene32851), *DXS* (MS.gene96182) and *GGDS* (MS.gene87404/28490), showed upward trend by salinity treatment in roots and/or leaves in GIB, while in LS, they showed downward trend (Table S11). Furthermore, *DXS*, *HDR* in roots and *SQE1* in leaves showed higher expression in salinity-tolerant variety GIB than in salinity-sensitive variety LS under salinity stress condition (Table S11). Increasing evidence suggests that terpenoid-derived metabolites contribute to stress adaptation through multiple physiological mechanisms (Ramos et al. 2009; Younis et al. 2024). For instance, saponin has been reported to alleviate salinity stress by promoting root growth, modulating plant hormone levels, and stimulating antioxidant activity (Younis et al. 2024). *DXS* encodes the first rate-limiting enzyme of the plastidial MEP pathway to synthesize terpenoids, which has been proved to be related to enhancing tolerance against both biotic and abiotic stresses (Wei et al. 2019; Zhao et al. 2024). Overexpression of *PtDXS* gene in Populus Nanlin895 increased resistance to *S.*

populiperda infection by modulating ABA and gibberellic acid accumulation (Wei et al. 2019). Similarly, transgenic tobacco plants overexpressing *DfDXS1* and *DfDXS2* genes displayed enhanced tolerance to both salinity and drought stress (Zhao et al. 2024). HDR is key enzyme that regulate the isopentenyl pyrophosphate and dimethylallyl diphosphate biosynthesis by the plastidial MEP pathway. A mutation of *HDR* in *A. thaliana* was reported to lead to the decrease of chlorophyll content (Hsieh and Goodman. 2005). In addition, the *DsHDR* gene has been proposed to participate in carotenoid biosynthesis, and thus it has a high transcription level in *Dunaliella salina* cells under nutrient depletion, high salinity and/or strong light conditions (Ramos et al. 2009). Saponin is a kind of glycoside with triterpenoid or spirostane aglycone, and SQE is the key enzyme for sterol and saponin biosynthesis by the cytoplasmic MVA pathway (Jaramillo-Madrid et al. 2020; Kang et al. 2019; Kaushal et al. 2023). Meanwhile, an exogenous application of saponin was shown to alleviate the inhibitory effects of salinity during quinoa seed germination (Yang et al. 2018). These results showed that *DXS, HDR* and *SQE1* genes may serve as critical contributors to salinity stress adaptation in alfalfa salinity-tolerant variety GIB.

4.2.3 DEGs involved in metabolic pathway of nitrogen-containing compounds (Alkaloids and Polyamines)

Alkaloids, as nitrogen-containing plant secondary metabolites, mainly include isoquinoline alkaloids, pyrrolidine alkaloids and indole alkaloids, which play crucial roles in plant stress tolerance (Gaude and Jalmi 2025; Hassan et al. 2021). In this study, 113 DEGs encoding 5 enzyme families (G8H, STR, TRI, TAT and TYDC)

involved in the biosynthesis of isoquinoline alkaloid, pyrrolidine alkaloids and indole alkaloids were identified in GIB variety following salinity treatment (Table S9). Among them, 22 genes were significantly upregulated in at least two pairwise comparisons in roots and/or leaves (Table S10 and Figure 6). Importantly, 17 genes, including *G8H* (MS.gene005805/005807/006077/010726/037889/066931/ 60535), *STR4* (MS.gene64464), *TRI* (MS.gene30551/41122/46110), *TYDC1* (MS.gene003256/02053/03160), and *TAT2* (MS.gene032280/34230/36049), showed upward trend by salinity treatment in roots and/or leaves in GIB, while in LS, they showed downward trend (Table S11). G8H and STR are recognized as pivotal enzymes in the biosynthetic pathway of terpenoids indole alkaloids (Ramadan et al. 2020). Overexpression of *PgCYP76C9* gene enhances *Pseudomonas syringae* resistance in transgenic *Arabidopsis* by improving the terpenoid indole alkaloid accumulation (Balusamy et al. 2017). Moreover, it has been reported that foliar spray of salicylic acid enhances the resistance to salinity by improving the content of the terpenoids indole alkaloids (Idrees et al. 2011). Here, *G8H* (MS.gene066931), *STR4* (MS.gene64464) genes in roots, and *G8H* (MS.gene010726/037889) genes in leaves showed higher expression in salinity-tolerant variety GIB than in salinity-sensitive variety LS under salinity treatment (Table S11), implying that *G8H* and *STR4* genes might be critical factors in contributing to resistance to salinity in salinity-tolerant variety GIB. TRI catalyzes the reduction of tropinone to tropine and is considered a key enzyme in the biosynthesis of tropane alkaloids (Hu et al. 2023b), which represent an important subgroup of the pyrrolidine alkaloids (Kim et al. 2016). Under salinity

stress condition, *TRI* (MS.gene46110) gene in roots showed higher expression in salinity-tolerant variety GIB than in salinity-sensitive variety LS (Table S11). However, so far, there is no report that tropane alkaloids could improve the plants salinity tolerance, so the function of *TRI* gene requires further verification. TYDC and TAT catalyze the conversion of tyrosine into dopamine and 4-hydroxyphenylacetaldehyde, respectively, representing the initial committed reactions in isoquinoline alkaloid biosynthesis (Mishra et al. 2013). Previous studies have shown that overexpression of *MdTYDC* enhances salinity tolerance in transgenic *Malus domestica* by increasing the contents of dopamine and proline, as well as antioxidant enzyme activities and maintained ion homeostasis (Gao et al. 2021; Wang et al. 2020). Similarly, *PaTYDC4* has been reported to improve drought resistance in transgenic poplars through enhanced xylem differentiation and lignin deposition (Wang et al. 2025a). In this study, *TAT2* in roots, and *TYDC1* (MS.gene003256/03160) in leaves, exhibited higher expression in salinity-tolerant variety GIB than in salinity-sensitive variety LS under salinity stress condition (Table S11). These results suggested that *TYDC1* gene might be critical factors in contributing to resistance to salinity in salinity-tolerant variety GIB. Meanwhile, the function of *TAT2* gene remains uncharacterized, requiring further investigation.

Polyamines, including putrescine, spermidine, and spermine, are well-known regulators of plant responses to environmental stresses and have been extensively associated with salinity tolerance (Amiri et al. 2024; Qaderi et al. 2023). In this study, 56 DEGs encoding 6 enzyme families (ADC, ODC, PAO, SAMDC, SAMS and SPDS)

involved in polyamine biosynthesis were identified in GIB under salinity stress (Table S9). Among them, 13 genes were upregulated in at least two pairwise comparisons in roots and/or leaves (Table S10 and Figure 6). Notably, ten genes, including *SAMS* (MS.gene050426/26796), *SAMS3* (MS.gene22399/007396/47449), *SAMDC* (MS.gene022054), *ADC* (MS.gene23355), and *PAO5* (MS.gene026071/21960/85388), exhibited increased expression in GIB following salinity treatment but showed opposite expression trends in LS (Table S11). SAMS catalyzes the synthesis of S-adenosylmethionine, a crucial precursor for polyamine production (Hu et al. 2023a). Overexpression of *MfSAMS1* has been shown to improve chilling tolerance in transgenic stylo, likely through regulation of polyamine metabolism (Qiu et al. 2019). Likewise, heterologous expression of *CsSAMS1* increased salinity tolerance in *Escherichia coli* BL21 (He et al. 2019). In this study, *SAMS* (MS.gene050426/26796) and *SAMS3* (MS.gene22399/007396/47449) showed higher expression in leaves of salinity-tolerant variety GIB than in salinity-sensitive variety LS under salinity stress condition (Table S11), indicating that *SAMS* genes might be critical factors in contributing to resistance to salinity in salinity-tolerant variety GIB. PAOs are flavin adenine dinucleotide-dependent enzymes that catalyze conversion of spermine to spermidine, and spermidine to putrescine, and play a crucial roles in stress tolerance in plant (Amiri et al. 2024; Qaderi et al. 2023). For example, overexpression of *CsPAO3* in *A. thaliana* promoted seed germination and root growth following salinity treatment (Wu et al. 2022), as well as transgenic rice expressing *OsPAO3* exhibited enhanced salinity tolerance in the germination stage (Liu et al. 2022). Here, *SAMS*,

SAMS3 and *PAO5* (MS.gene026071/21960/85388) showed higher expression in leaves of salinity-tolerant variety GIB than in salinity-sensitive variety LS under salinity stress condition (Table S11). Collectively, these findings indicated that *PAO5* might be critical factor in contributing to salinity stress adaptation in alfalfa salinity-tolerant variety GIB.

5 Conclusion

In time-course transcriptome analysis of salinity-tolerant variety GIB at 0, 24 and 72 hours after 200 mM NaCl treatment, a total of 16,457, 14,527, 16,967, 18,210, 12,887 and 14,838 DEGs were identified in R_{24}/R_0, R_{72}/R_0, R_{72}/R_{24}, L_{24}/L_0, L_{72}/L_0 and L_{72}/L_{24}, respectively. Of them, 521 DEGs related to biosynthesis of secondary metabolites, including phenolic compounds (276), terpenoid compounds (76), and nitrogen-containing compounds (169), were identified. Through combined analysis of comparative transcriptome between salinity-tolerant variety GIB and salinity-sensitive variety LS, interestingly, several genes involved in phenolic compounds biosynthesis (*4CLL9*, *ANR*, *UFGT7*, *CSE*, *COMT1*), terpenoid compounds biosynthesis (*HDR*, *SQE1*, *DXS*), and nitrogen-containing compounds biosynthesis (*G8H, STR4, TRI, TAT2, TYDC1, SAMSs,* and *PAO5*) exhibited higher expression levels in roots and/or leaves of the salinity-tolerant variety GIB than in the salinity-sensitive variety LS under salinity stress condition. These genes are therefore proposed as candidates involved in the regulation of salinity tolerance of GIB. These findings provide valuable insights for the contribution of secondary metabolic pathway to salinity adaptation of alfalfa, and lay a foundation for cultivating salinity-tolerant alfalfa varieties through molecular breeding in the future.

Declarations

Abbreviations

GIB: Alfalfa variety Gibraltar

LS: Alfalfa variety LS1405

TPM: Transcripts Per Million

FDR: False discovery rate

DEG: Differentially expressed gene

GO: Gene ontology

KEGG: Kyoto encyclopedia of genes and genomes

BLAST: Basic Local Alignment Search Tool

RT-qPCR: Reverse-transcription quantitative PCR

FPKM: Fragments Per Kilobase of transcript per Million mapped fragments

ANOVA: Analysis of variance

MEP: Methylerythritol phosphate

MVA: Mevalonate

Ethics approval and consent to participate

Not applicable.

Consent for publication

Not applicable.

Data availability

The raw data supporting the conclusions of this article have been deposited in the Genome Sequence Archive at Beijing Institute of Genomics (China National Center for Bioinformation) (GSA: CRA037503, https://ngdc.cncb.ac.cn/gsa).

Competing Interests

The authors declare no conflicts of interest.

Funding

This research was funded by the Key Research and Development Program of Shandong Province (2026LZGC035); China Agriculture Research System (CARS-33); the Huaibei Normal University Re-established Project (2024ZK38).

Authors' contributions

Guoliang Wang, Xueling Du, Rugang Yu conceived and designed the experiments. Rugang Yu, Na Wu and Lin Yang wrote the manuscript and performed the data analyses. Lin Yang, Na Wu, Yanan Gu, Minyi Liu, Hanyu Ma, Xiaona Niu conducted experiment and analyzed data. Guoliang Wang, Xueling Du revised the manuscript. All authors read and approved the final manuscript.

Acknowledgements

Not applicable.

Reference

Acharya BR, Gill SP, Kaundal A et al (2024) Strategies for combating plant salinity stress: the potential of plant growth-promoting microorganisms. Frontiers in Plant Science 15: 1406913. https://doi.org/10.3389/fpls.2024.1406913

Ahmad I, Zhu G, Zhou G et al (2023) Integrated approaches for increasing plant yield under salt stress. Front. Plant Sci. 14:1215343. doi: 10.3389/fpls.2023.1215343

Amiri H, Banakar MH, Hemmati Hassan Gavyar P (2024) Polyamines: new plant growth regulators promoting salt stress tolerance in plants. J Plant Growth Regul 43:4923–4940. https://doi.org/10.1007/s00344-024-11447-z

An Y, Suo X, Niu Q et al (2022) Genome-wide identification and analysis of the NF-Y transcription factor family reveal its potential roles in salt stress in alfalfa (Medicago sativa L.). Int J Mol Sci 23(12):6426. https://doi.org/10.3390/ijms23126426

Balusamy SRD, Rahimi S, Cho YG et al (2017) Overexpression of geraniol 10-hydroxylase from Panax ginseng conferred enhanced resistance to Pseudomonas syringae in Arabidopsis. Plant Growth Regul 81:305–316. https://doi.org/10.1007/s10725-016-0207-6

Ben-Dor A, Steiner M, Gheber L et al (2005) Carotenoids activate the antioxidant response element transcription system. Mol Cancer Ther 4(1):177–186. https://doi.org/10.1158/1535-7163.177.4.1

Białek W, Czechowicz P, Grzyb J et al (2026) Plant flavonoid effects on the non-apoptotic mechanisms of regulated cell death. Phytochem Rev 25:597–641. https://doi.org/10.1007/s11101-025-10140-7

Chang J, Guo Y, Yan J et al (2021) The role of watermelon caffeic acid O-methyltransferase (ClCOMT1) in melatonin biosynthesis and abiotic stress tolerance. Hortic Res 8(1):210. https://doi.org/10.1038/s41438-021-00645-5

Gao T, Wang Y, Liu Y et al (2021) Overexpression of tyrosine decarboxylase (MdTYDC) enhances drought tolerance in Malus domestica. Sci Hortic 289:110425. https://doi.org/10.1016/j.scienta.2021.110425

Gaude AA, Jalmi SK (2025) Environmental stress induced biosynthesis of plant secondary metabolites-transcriptional regulation as a key. Crop Des 4(2):100100. https://doi.org/10.1016/j.cropd.2025.100100

Ge L, Yang X, Liu Y et al (2023) Improvement of seed germination under salt stress via overexpressing caffeic acid O-methyltransferase 1 (SlCOMT1) in Solanum lycopersicum L. Int J Mol Sci 24(1):734. https://doi.org/10.3390/ijms24010734

Hassan FAS, Ali E, Gaber A et al (2021) Chitosan nanoparticles effectively combat salinity stress by enhancing antioxidant activity and alkaloid biosynthesis in Catharanthus roseus (L.) G. Don. Plant Physiol Biochem 162:291–300. https://doi.org/10.1016/j.plaphy.2021.03.004

He MW, Wang Y, Wu JQ et al (2019) Isolation and characterization of S-adenosylmethionine synthase gene from cucumber and responsive to abiotic stress. Plant Physiol Biochem 141:431–445. https://doi.org/10.1016/j.plaphy.2019.06.006

He S, Ye Y, Yuan Y et al (2023) Insights into flavonoid biosynthesis during cucumber fruit peel coloration based on metabolite profiling and transcriptome analyses. Hortic Plant J 9(4):763–776. https://doi.org/10.1016/j.hpj.2023.02.002

Hsieh MH, Goodman HM (2005) The Arabidopsis IspH homolog is involved in the plastid nonmevalonate pathway of isoprenoid biosynthesis. Plant Physiol 138(2):641–653. https://doi.org/10.1104/pp.104.058735

Hu W, Hu S, Li S et al (2023a) AtSAMS regulates floral organ development by DNA methylation and ethylene signaling pathway. Plant Sci 334:111767. https://doi.org/10.1016/j.plantsci.2023.111767

Hu X, Liu W, Yan Y et al (2023b) Tropinone reductase: a comprehensive review on its role as the key enzyme in tropane alkaloids biosynthesis. Int J Biol Macromol 253(Pt 7):127377. https://doi.org/10.1016/j.ijbiomac.2023.127377

Idrees M, Naeem M, Aftab T et al (2011) Salicylic acid mitigates salinity stress by improving antioxidant defence system and enhances vincristine and vinblastine alkaloids production in periwinkle [Catharanthus roseus (L.) G. Don]. Acta Physiol Plant 33(3):987–999. https://doi.org/10.1007/s11738-010-0631-6

Jaramillo-Madrid AC, Abbriano R, Ashworth J et al (2020) Overexpression of key sterol pathway enzymes in two model marine diatoms alters sterol profiles in Phaeodactylum tricornutum. Pharmaceuticals 13(12):481. https://doi.org/10.3390/ph13120481

Jia J, Wang F, Yuan M et al (2025) Transcriptomic analysis reveals that the photosynthesis and carotenoid metabolism pathway is involved in the salinity stress response in Brassica rapa L. ssp. Pekinensis. Plants 14(4):566. https://doi.org/10.3390/plants14040566

Kang J, Zhang Q, Jiang X et al (2019) Molecular cloning and functional identification of a squalene synthase encoding gene from alfalfa (Medicago sativa L.). Int J Mol Sci 20(18):4499. https://doi.org/10.3390/ijms20184499

Kaushal N, Verma D, Alok A et al (2023) Heterologous expression of Chlorophytum borivilianum squalene epoxidase in tobacco modulates stigmasterol production and alters vegetative and reproductive growth. Plant Cell Rep 42(5):909–919. https://doi.org/10.1007/s00299-023-03000-1

Kim JY, Cho KH, Keene SA et al (2023) Altered profile of floral volatiles and lignin content by down-regulation of caffeoyl shikimate esterase in Petunia. BMC Plant Biol 23(1):210. https://doi.org/10.1186/s12870-023-04203-0

Kim N, Estrada O, Chavez B et al (2016) Tropane and granatane alkaloid biosynthesis: a systematic analysis. Molecules 21(11):1510. https://doi.org/10.3390/molecules21111510

Lavhale SG, Kalunke RM, Giri AP (2018) Structural, functional and evolutionary diversity of 4-coumarate-CoA ligase in plants. Planta 248(5):1063–1078. https://doi.org/10.1007/s00425-018-2965-z

Li C, Ji J, Wang G et al (2020) Over-expression of LcPDS, LcZDS, and LcCRTISO, genes from wolfberry for carotenoid biosynthesis, enhanced carotenoid accumulation, and salt tolerance in tobacco. Front Plant Sci 11:119. https://doi.org/10.3389/fpls.2020.00119

Liu G, Jiang W, Tian L et al (2022) Polyamine oxidase 3 is involved in salt tolerance at the germination stage in rice. J Genet Genomics 49(5):458–468. https://doi.org/10.1016/j.jgg.2022.01.007

Liu P, Li X, Zhao L et al (2025) Integrated transcriptome and metabolome analysis of salinity tolerance in chrysanthemum polyploids. Ind Crops Prod 236:121951. https://doi.org/10.1016/j.indcrop.2025.121951

Liu Q, Luo L, Zheng L (2018) Lignins: biosynthesis and biological functions in plants. Int J Mol Sci 19(2):335. https://doi.org/10.3390/ijms19020335

Luo P, Shen Y, Jin S et al (2016) Overexpression of Rosa rugosa anthocyanidin reductase enhances tobacco tolerance to abiotic stress through increased ROS scavenging and modulation of ABA signaling. Plant Sci 245:35–49. https://doi.org/10.1016/j.plantsci.2016.01.007

Ly LK, Ho TM, Bui TP et al (2024) CRISPR/Cas9 targeted mutations of OsDSG1 gene enhanced salt

tolerance in rice. Funct Integr Genomics 24(2):70. https://doi.org/10.1007/s10142-024-01347-6
Ma X, Umar AW, Zhou Y et al (2025) Hydroxycinnamoyl-CoA shikimate/quinate hydroxycinnamoyl transferase CtHCT061 enhances lignin biosynthesis and drought tolerance in safflower (Carthamus tinctorius L.). Ind Crops Prod 236:121929. https://doi.org/10.1016/j.indcrop.2025.121929
Mahmood T, Abdullah M, Ahmar S et al (2020) Incredible role of osmotic adjustment in grain yield sustainability under water scarcity conditions in wheat (Triticum aestivum L.). Plants 9(9):1208. https://doi.org/10.3390/plants9091208
Mishra S, Triptahi V, Singh S et al (2013) Wound induced transcriptional regulation of benzylisoquinoline pathway and characterization of wound inducible PsWRKY transcription factor from Papaver somniferum. PLoS One 8(1):e52784. https://doi.org/10.1371/journal.pone.0052784
Ni X, Wang Y, Dai L et al (2025) The transcription factor GmbZIP131 enhances soybean salt tolerance by regulating flavonoid biosynthesis. Plant Physiol 197(3):kiaf092. https://doi.org/10.1093/plphys/kiaf092
Nie T, Sun X, Wang S et al (2023) Genome-wide identification and expression analysis of the 4-coumarate: CoA ligase gene family in Solanum tuberosum. Int J Mol Sci 24(2):1642. https://doi.org/10.3390/ijms24021642
Pan F, Li H, Qu M et al (2025) Melatonin enhances salt tolerance by promoting CcCAD10-mediated lignin biosynthesis in pigeon pea. Theor Appl Genet 138(4):81. https://doi.org/10.1007/s00122-025-04846-7
Qaderi MM, Martel AB, Strugnell CA (2023) Environmental factors regulate plant secondary metabolites. Plants 12(3):447. https://doi.org/10.3390/plants12030447
Qiu H, Zhou M, Huang L et al (2019) Overexpression of MfSAMS1 improves chilling tolerance in transgenic stylo. Agron J 111(5):2287–2292. https://doi.org/10.2134/agronj2019.03.0192
Ramadan AM, Abdulgader MA, Khan T et al (2020) Differential expression of indole alkaloid pathway genes across Catharanthus roseus plant organs. Pak J Bot 52(4):1305–1313. https://doi.org/10.30848/pjb2020-4(34)
Ramos AA, Marques AR, Rodrigues M et al (2009) Molecular and functional characterization of a cDNA encoding 4-hydroxy-3-methylbut-2-enyl diphosphate reductase from Dunaliella salina. J Plant Physiol 166(9):968–977. https://doi.org/10.1016/j.jplph.2008.11.008
Sangabriel-Conde W, Maldonado-Mendoza IE, Mancera-López ME et al (2015) Glomeromycota associated with Mexican native maize landraces in Los Tuxtlas, Mexico. Appl Soil Ecol 87:63–71. https://doi.org/10.1016/j.apsoil.2014.10.017
Shrivastava P, Kumar R (2015) Soil salinity: a serious environmental issue and plant growth promoting bacteria as one of the tools for its alleviation. Saudi J Biol Sci 22(2):123–131. https://doi.org/10.1016/j.sjbs.2014.12.001
Song C, Acuña T, Adler-Agmon M et al (2022) Leveraging a graft collection to develop metabolome-based trait prediction for the selection of tomato rootstocks with enhanced salt tolerance. Hortic Res 9:uhac061. https://doi.org/10.1093/hr/uhac061
Waheed A, Zhuo L, Wang M et al (2024) Integrative mechanisms of plant salt tolerance: biological pathways, phytohormonal regulation, and technological innovations. Plant Stress 14:100652. https://doi.org/10.1016/j.stress.2024.100652

Wang Q, Wang Y, Lu X et al (2025a) Wood forming tissue-specific expression of PaTyDC4 promotes xylem differentiation and lignin deposition during secondary growth and confers drought tolerance in Populus. Hortic Plant J 11(2):854–864. https://doi.org/10.1016/j.hpj.2023.09.007

Wang Y, Gao T, Zhang Z et al (2020) Overexpression of the tyrosine decarboxylase gene MdTyDC confers salt tolerance in apple. Environ Exp Bot 180:104244. https://doi.org/10.1016/j.envexpbot.2020.104244

Wang Y, Teng B, Zhang H et al (2025b) Effects and mechanisms of Attapulgite Clay-g-(AA-co-AAm) hydrogel (ACH) in alleviating saline stress in spinach. Plants 14(21):3330. https://doi.org/10.3390/plants14213330

Wei H, Movahedi A, Xu C et al (2019) Overexpression of PtDXS enhances stress resistance in poplars. Int J Mol Sci 20(7):1669. https://doi.org/10.3390/ijms20071669

Wen H, Zhang S, Liu Y et al (2024) Screening universal stress-response terpenoids and their biosynthetic genes via volatile and transcriptomic profiling in citrus. J Agric Food Chem 72(1):351–362. https://doi.org/10.1021/acs.jafc.3c06109

Wu F, Qu D, Zhang X et al (2023) PaLectinL7 enhances salt tolerance of sweet cherry by regulating lignin deposition in connection with PaCAD1. Tree Physiol 43(11):1986–2000. https://doi.org/10.1093/treephys/tpad099

Wu J, Liu W, Jahan MS et al (2022) Characterization of polyamine oxidase genes in cucumber and roles of CsPAO3 in response to salt stress. Environ Exp Bot 194:104696. https://doi.org/10.1016/j.envexpbot.2021.104696

Wu J, Wang X, Xu J et al (2026) Overexpression of soybean flavonoid 3′-hydroxylase enhances plant salt tolerance by promoting ascorbic acid biosynthesis. J Adv Res 80:111–123. https://doi.org/10.1016/j.jare.2025.05.009

Yang A, Akhtar SS, Iqbal S et al (2018) Saponin seed priming improves salt tolerance in quinoa. J Agron Crop Sci 204(1):31–39. https://doi.org/10.1111/jac.12229

Yang G, Li Z, Rong M et al (2024) Comparative transcriptome analysis to identify the important mRNA and lncRNA associated with salinity tolerance in alfalfa. PeerJ 12:e18236. https://doi.org/10.7717/peerj.18236

Yang L, Sun Q, Geng B et al (2023) Jasmonate biosynthesis enzyme allene oxide cyclase 2 mediates cold tolerance and pathogen resistance. Plant Physiol 193(2):1621–1634. https://doi.org/10.1093/plphys/kiad362

Yang X, Qin H, Zhou Y et al (2025) HB52-PUT2 module-mediated polyamine shoot-to-root movement regulates salt stress tolerance in tomato. Plant Cell Environ 48(7):5148–5163. https://doi.org/10.1111/pce.15479

Yin Y, Yang T, Li S et al (2023) Transcriptomic analysis reveals that methyl jasmonate confers salt tolerance in alfalfa by regulating antioxidant activity and ion homeostasis. Front Plant Sci 14:1258498. https://doi.org/10.3389/fpls.2023.1258498

Younis U, Danish S, Datta R et al (2024) Synergistic effects of boron and saponin in mitigating salinity stress to enhance sweet potato growth. Sci Rep 14(1):12988. https://doi.org/10.1038/s41598-024-63840-z

Yu R, Chen X, Zhang H et al (2025) Development of SSR markers related to salinity resistance based on transcriptomic sequences in Medicago sativa. PLoS One 20(11):e0336528. https://doi.org/10.1371/journal.pone.0336528

Yu R, Wang G, Yu X et al (2021) Assessing alfalfa (Medicago sativa L.) tolerance to salinity at seedling stage and screening of the salinity tolerance traits. Plant Biol 23(4):664–674. https://doi.org/10.1111/plb.13271

Yu Z, Niu L, Cai Q et al (2023) Improved salt-tolerance of transgenic soybean by stable over-expression of AhBADH gene from Atriplex hortensis. Plant Cell Rep 42(8):1291–1310. https://doi.org/10.1007/s00299-023-03031-8

Zhan W, Cui L, Song N et al (2025) Comprehensive analysis of cinnamoyl-CoA reductase (CCR) gene family in wheat: implications for lignin biosynthesis and stress responses. BMC Plant Biol 25(1):567. https://doi.org/10.1186/s12870-025-06605-8

Zhang K, Sun Y, Li M et al (2021) CrUGT87A1, a UDP-sugar glycosyltransferases (UGTs) gene from Carex rigescens, increases salt tolerance by accumulating flavonoids for antioxidation in Arabidopsis thaliana. Plant Physiol Biochem 159:28–36. https://doi.org/10.1016/j.plaphy.2020.12.006

Zhang Y, Diao S, Ding X et al (2023) Transcriptional regulation modulates terpenoid biosynthesis of Pinus elliottii under drought stress. Ind Crops Prod 202:116975. https://doi.org/10.1016/j.indcrop.2023.116975

Zhao D, Luan Y, Shi W et al (2021) A Paeonia ostii caffeoyl-CoA O-methyltransferase confers drought stress tolerance by promoting lignin synthesis and ROS scavenging. Plant Sci 303:110765. https://doi.org/10.1016/j.plantsci.2020.110765

Zhao H, Su J, Zhong Z et al (2024) Functional identification and regulatory active site screening of the DfDXS gene of Dryopteris fragrans. Plants 13(18):2647. https://doi.org/10.3390/plants13182647

Zhou H, Meng F, Jiang W et al (2024) Potassium indole-3-butyric acid affects rice's adaptability to salt stress by regulating carbon metabolism, transcription factor genes expression, and biosynthesis of secondary metabolites. Front Plant Sci 15:1416936. https://doi.org/10.3389/fpls.2024.1416936

Zhu X, Yang Y, Fu Y et al (2026) Transcriptome-metabolome integration uncovers salt stress effects on flavonoid biosynthesis in two self-selected breeding alfalfa varieties. Physiol Plant 178(1):e70728. https://doi.org/10.1111/ppl.70728

Zhu Y, Wang Q, Wang Y et al (2021) Combined transcriptomic and metabolomic analysis reveals the role of phenylpropanoid biosynthesis pathway in the salt tolerance process of Sophora alopecuroides. Int J Mol Sci 22(5):2399. https://doi.org/10.3390/ijms22052399

Table captions

TABLE 1 Significantly enriched KEGG pathways for the DEGs in roots and leaves in all comparisons.

867 **TABLE 1** Significantly enriched KEGG pathways for the DEGs in roots and/or leaves in all comparisons.

Pathway term	DEGs tested			P_{adj}-value			DEGs tested			P_{adj}-value			Pathway ID
	R_{24}/R_0	R_{72}/R_0	R_{72}/R_{24}	R_{24}/R_0	R_{72}/R_0	R_{72}/R_{24}	L_{24}/L_0	L_{72}/L_0	L_{72}/L_{24}	L_{24}/L_0	L_{72}/L_0	L_{72}/L_{24}	
Phenylpropanoid biosynthesis	221	168	240	1.84E-26	1.15E-12	1.56E-31	143	111	119	0.019973608	0.009092269	0.056132162	ko00940
Nitrogen metabolism	58	33	53	4.67E-15	0.000593863	2.22E-11	37	23	12	0.001144869	0.081761932	1	ko00910
Biosynthesis of various plant secondary metabolites	90	72	99	1.86E-09	1.26E-05	7.81E-12	61	38	50	0.139815554	0.678633466	0.271175876	ko00999
MAPK signaling pathway - plant	164	135	177	1.99E-08	6.36E-05	2.58E-10	155	133	137	0.000651052	1.74E-06	0.000570911	ko04016
Starch and sucrose metabolism	180	149	171	9.05E-08	0.000187074	4.70E-05	178	129	117	0.000316234	0.002933894	0.549908052	ko00500
Linoleic acid metabolism	44	33	41	3.15E-06	0.003575393	9.13E-05	34	18	22	0.024786466	0.638493446	0.478234547	ko00591
Cutin, suberine and wax biosynthesis	41	33	43	0.000467787	0.016867294	0.000178324	34	21	29	0.076053617	0.543023181	0.111859767	ko00073
Cyanoamino acid metabolism	70	67	85	0.002213069	0.000682712	1.72E-06	43	28	35	1	1	1	ko00460
Tropane, piperidine and pyridine alkaloid biosynthesis	41	51	57	0.00314475	9.45E-08	2.52E-08	54	32	44	6.02E-06	0.022665073	0.000424882	ko00960
Isoflavonoid biosynthesis	41	54	75	0.011893726	1.15E-07	5.27E-15	40	31	36	0.069046853	0.085077001	0.056225549	ko00943
Flavonoid biosynthesis	65	71	88	0.028013262	0.000189287	8.51E-07	64	52	57	0.166208336	0.077734339	0.109526897	ko00941
Circadian rhythm - plant	42	64	56	0.048495485	6.00E-10	4.87E-05	41	37	48	0.176588858	0.028160373	0.001983491	ko04712
Glutathione metabolism	125	79	136	3.65E-08	0.282191909	3.63E-10	120	94	100	0.000182665	9.94E-05	0.001804051	ko00480
Cysteine and methionine metabolism	118	75	128	3.51E-06	0.510127682	9.70E-08	122	79	96	0.000127284	0.036650508	0.006990249	ko00270
Amino sugar and nucleotide sugar metabolism	131	100	144	0.000120173	0.13301354	2.53E-06	140	113	119	0.000668192	6.50E-05	0.002357614	ko00520
Galactose metabolism	44	52	80	0.287628582	0.005937076	1.80E-09	59	44	54	0.014283145	0.030744095	0.00574025	ko00052
Ribosome	140	268	253	1	1.26E-12	8.68E-05	249	240	427	0.015321304	5.27E-11	2.43E-66	ko03010
Phenylalanine metabolism	31	30	47	0.315227597	0.347285311	0.000340276	57	32	37	3.19E-06	0.037565453	0.026103062	ko00360
Carbon fixation in photosynthetic organisms	39	34	47	1	1	0.63556885	83	53	56	2.80E-06	0.007371664	0.025043136	ko00710
Carotenoid biosynthesis	32	16	27	0.190019259	1	0.777446477	56	39	37	2.93E-06	0.000439124	0.016794821	ko00906

868 Note: The red background indicates that the KEGG pathway is significantly enriched.

869 **Figure captions**

870 **FIGURE 1** Analysis of differentially expressed genes following 0, 24 and 72 h of
871 treatment with 200 mM NaCl in GIB variety. (A) The total number of up-regulated
872 and down-regulated genes. (B) Venn diagrams of up-regulated genes. (C) Venn
873 diagrams of down-regulated genes.

874 **FIGURE 2** The top 20 significantly enriched GO terms in each pairwise comparison.
875 (A) R_{24}/R_0, (B) R_{72}/R_0, (C) R_{72}/R_{24}, (D) L_{24}/L_0, (E) L_{72}/L_0, (F) L_{72}/L_{24}.

876 **FIGURE 3** The top 20 significantly enriched KEGG pathways in each pairwise
877 comparison. (A) R_{24}/R_0, (B) R_{72}/R_0, (C) R_{72}/R_{24}, (D) L_{24}/L_0, (E) L_{72}/L_0, (F) L_{72}/L_{24}.

878 **FIGURE 4** DEGs associated with metabolic pathway of phenolic compounds. The
879 gene with red font indicates the upregulated in at least two pairwise comparisons of
880 roots or leaves.

881 **FIGURE 5** DEGs associated with metabolic pathway of terpenoid compounds. The
882 gene with red font indicates the upregulated in at least two pairwise comparisons of
883 roots or leaves.

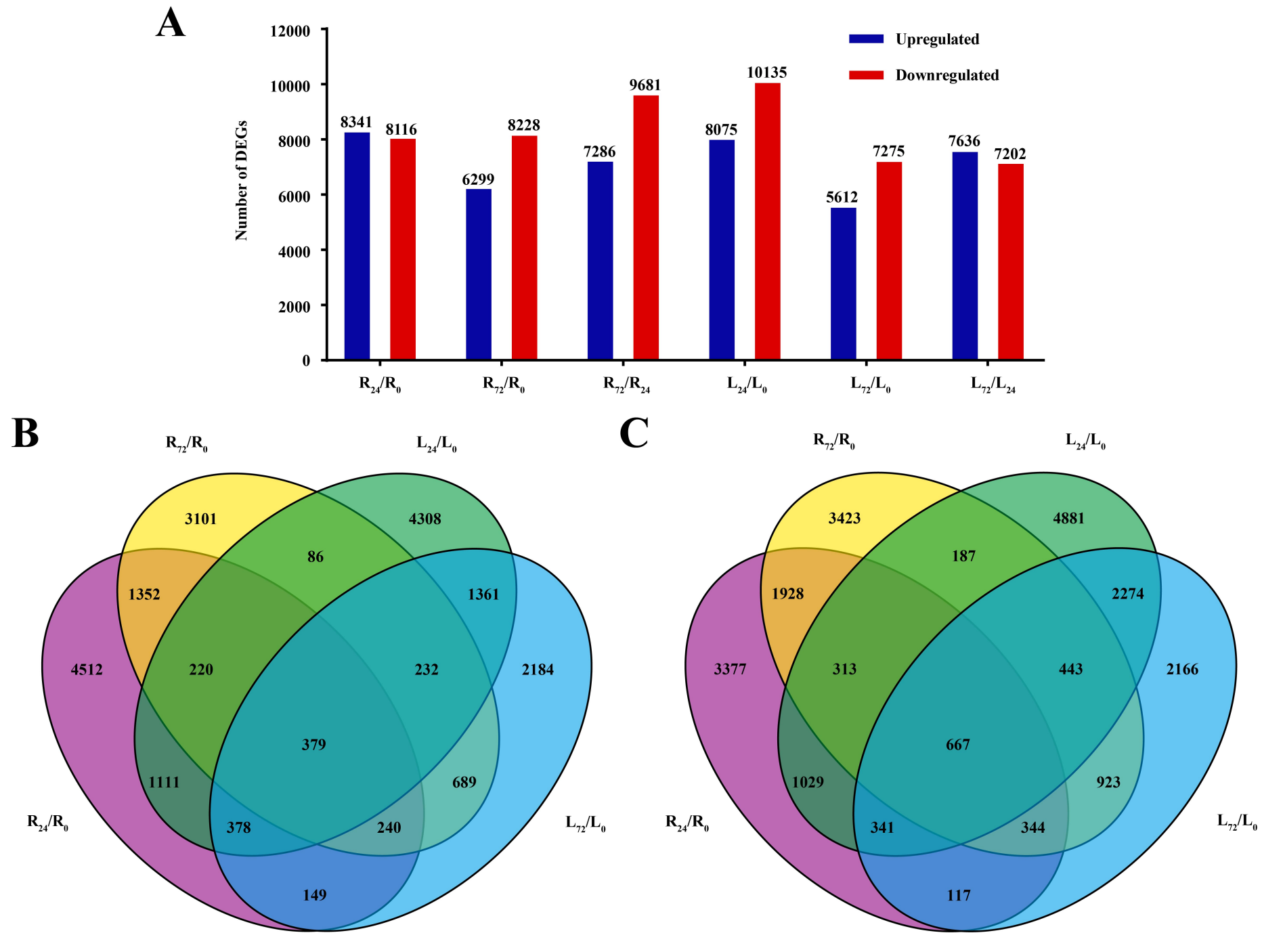
884 **FIGURE 6** DEGs associated with metabolic pathway of nitrogen-containing
885 compounds. The gene with red font indicates the upregulated in at least two pairwise
886 comparisons of roots or leaves.

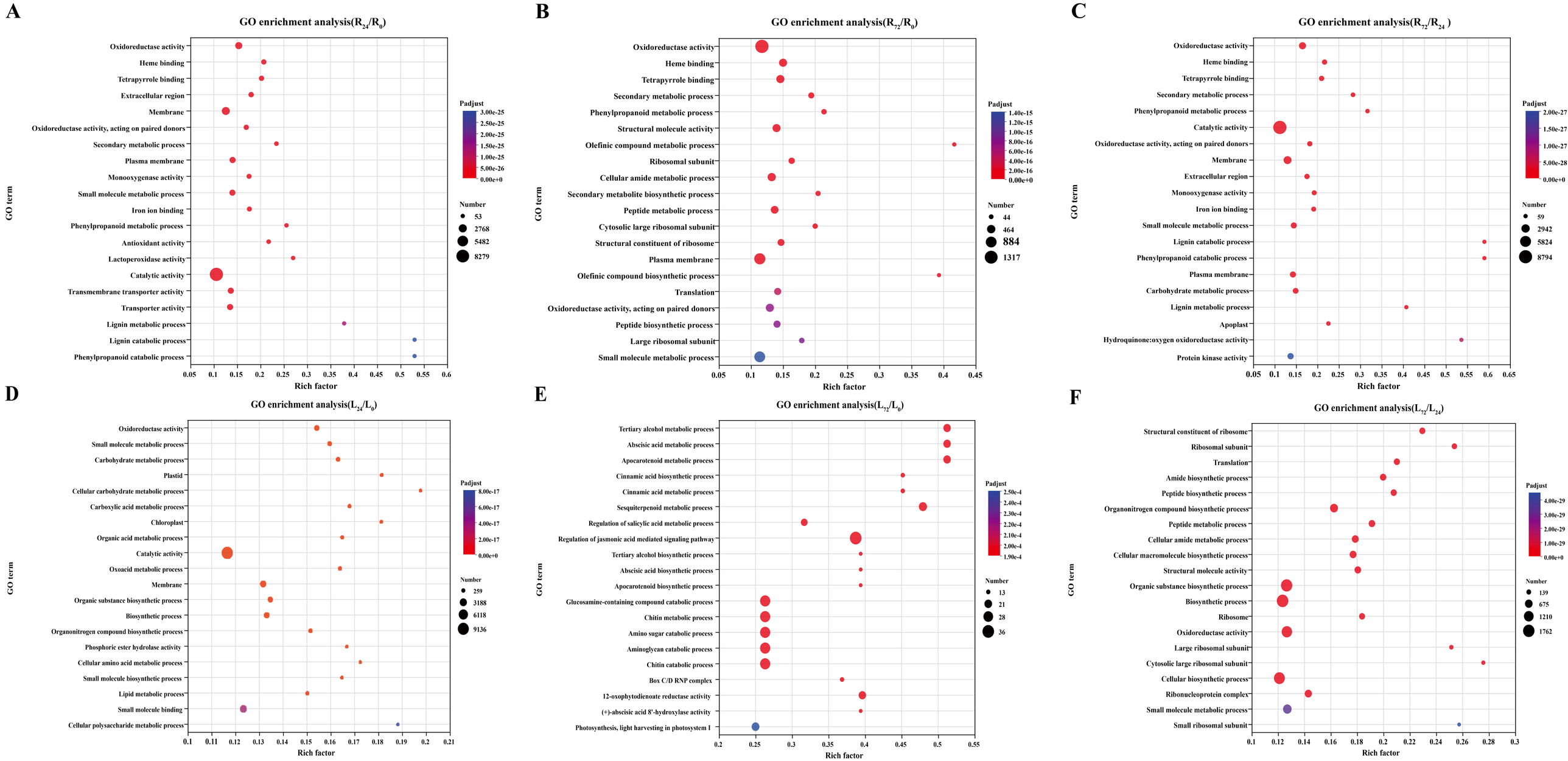
887 **FIGURE 7** RT-qPCR analyses of 10 candidate DEGs after 0, 24 and 72 h of
888 treatment with 200 mM NaCl in in roots (A) and leaves (B) of GIB variety. Each bar
889 represents the mean ± SD of triplicate assays. Different letters above the bars indicate
890 significant difference at the 0.05 level according to Duncan's multiple range test.

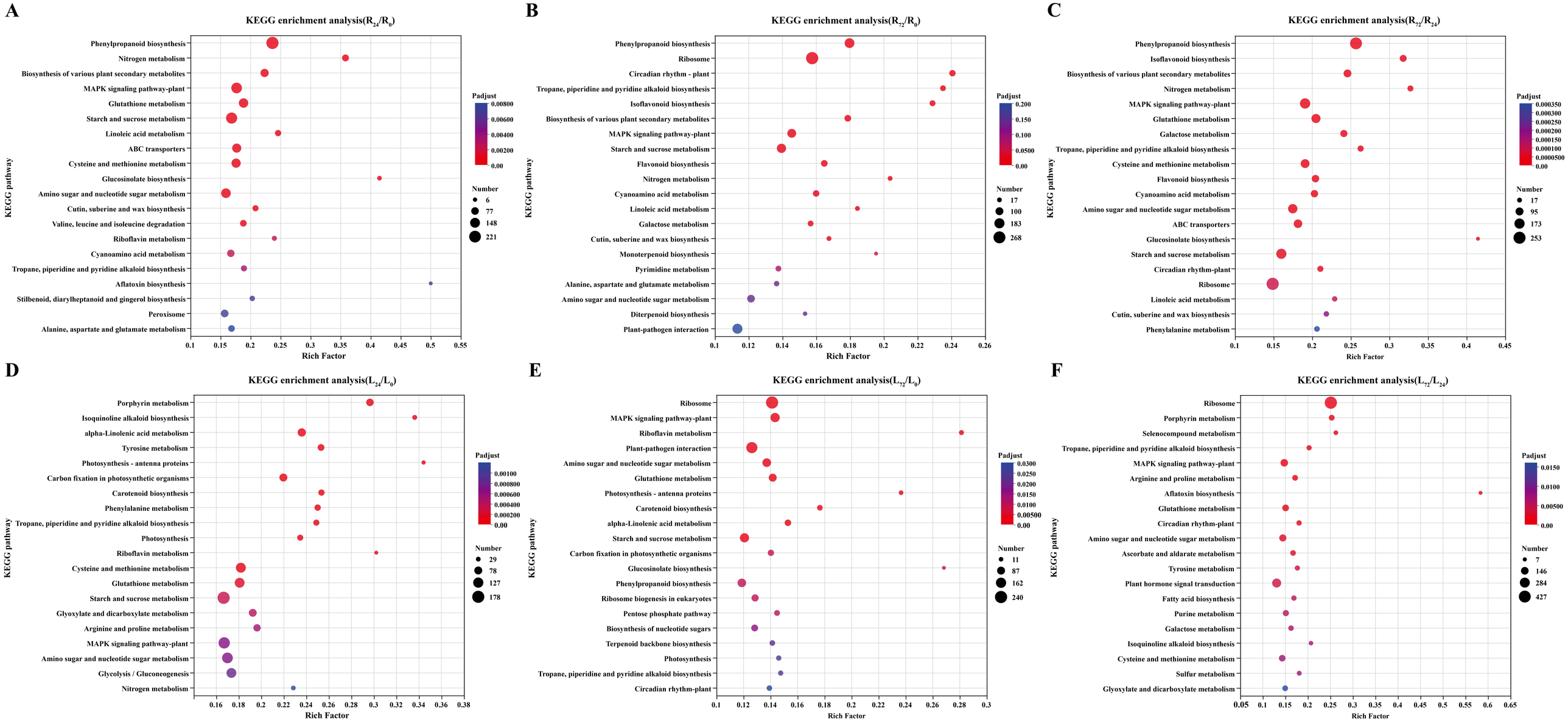
FIGURE 8 Correlation analysis of gene expression between RNA-seq data and RT-qPCR results. Transcriptome data were plotted against data from RT-qPCR. Data are presented on a $\log_2$(Fold change).

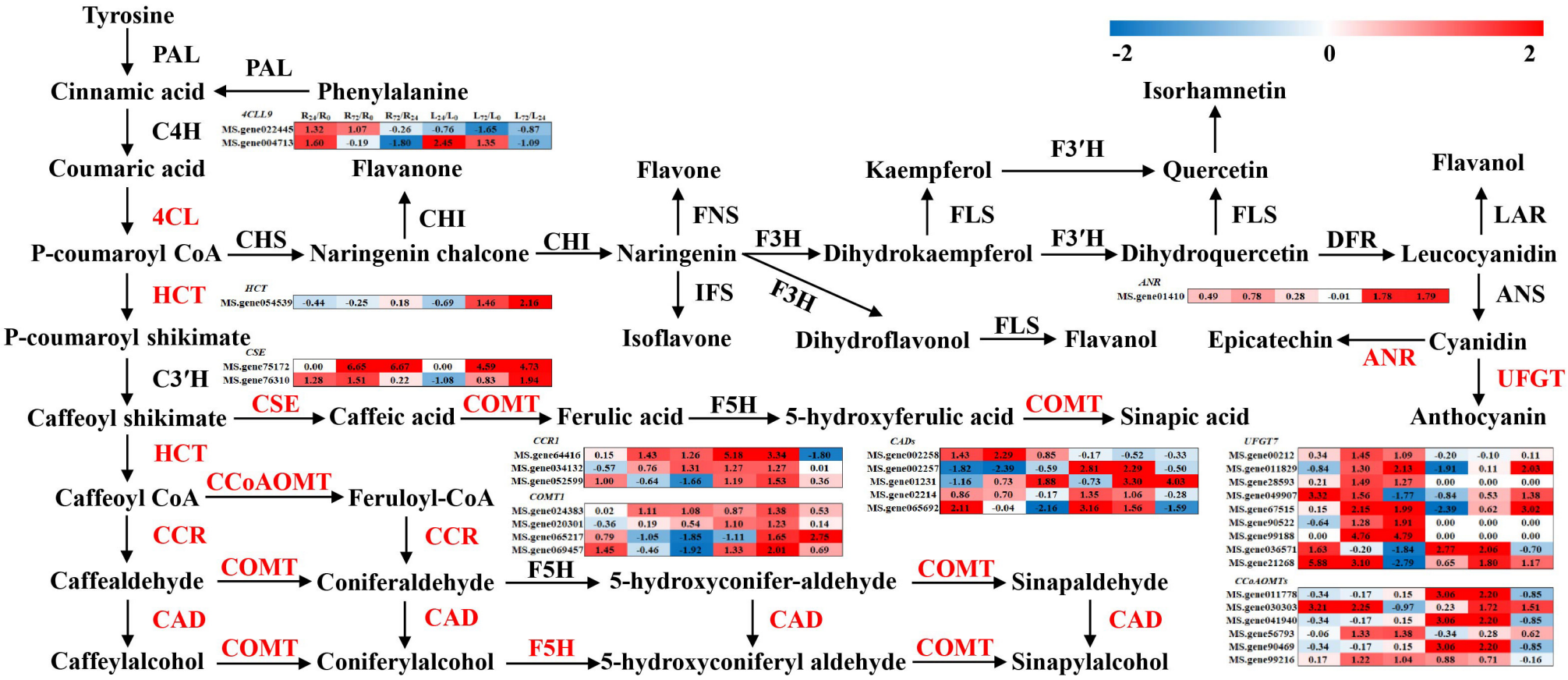
Supporting Information

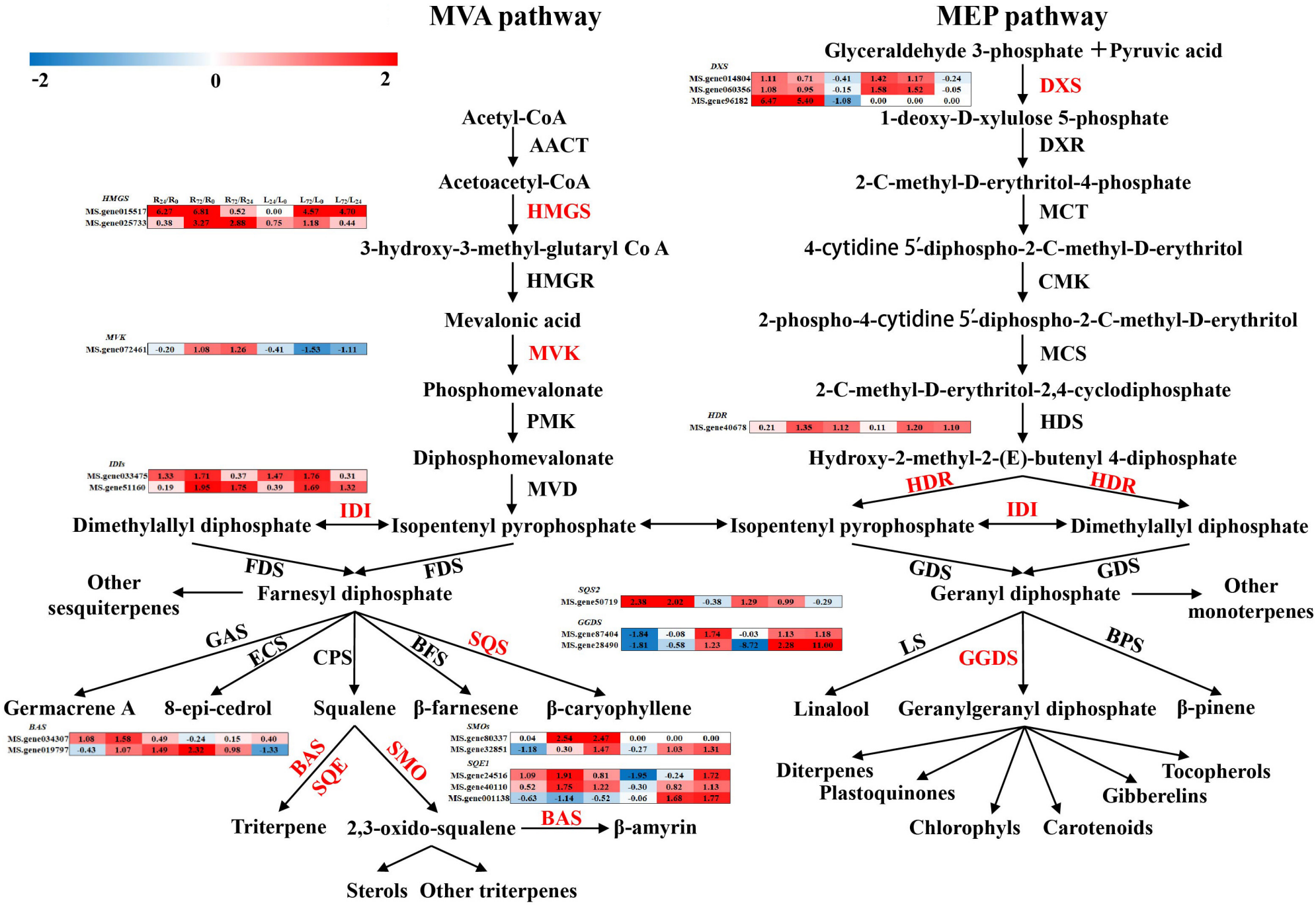
Additional supporting information can be found online in the Supporting Information section. **Table S1.** Primers used for RT-qPCR analysis. **Table S2.** Overview of raw and clean reads in GIB variety after 0, 24 and 72 h of treatment with 200 mM NaCl. **Table S3.** List of differentially expressed genes (DEGs) in six groups based on pairwise comparisons. **Table S4.** The enriched GO terms of all DEGs in the paired comparison of roots or leaves. **Table S5.** The GO terms of DEGs were shared significantly enriched in the paired comparison of roots or leaves. **Table S6.** Overview of all 133 KEGG pathways for DEGs in the paired comparison of roots or leaves. **Table S7.** Differentially expressed genes involved in metabolic pathway of phenolic compounds. **Table S8.** Differentially expressed genes involved in metabolic pathway of terpenoid compounds. **Table S9.** Differentially expressed genes involved in metabolic pathway of nitrogen-containing compounds. **Table S10.** Association profiling of the secondary metabolic pathway related-DEGs in roots and leaves in the time-course transcriptome sequencing data of GIB and the comparative transcriptome sequencing data between GIB and LS. **Table S11.** Genes related to secondary metabolic pathways in roots or leaves have the same up-regulated expression trends by salt stress in time-course transcriptome sequencing of GIB and comparative transcriptome sequencing of GIB and LS. (XLSX 12764kb)

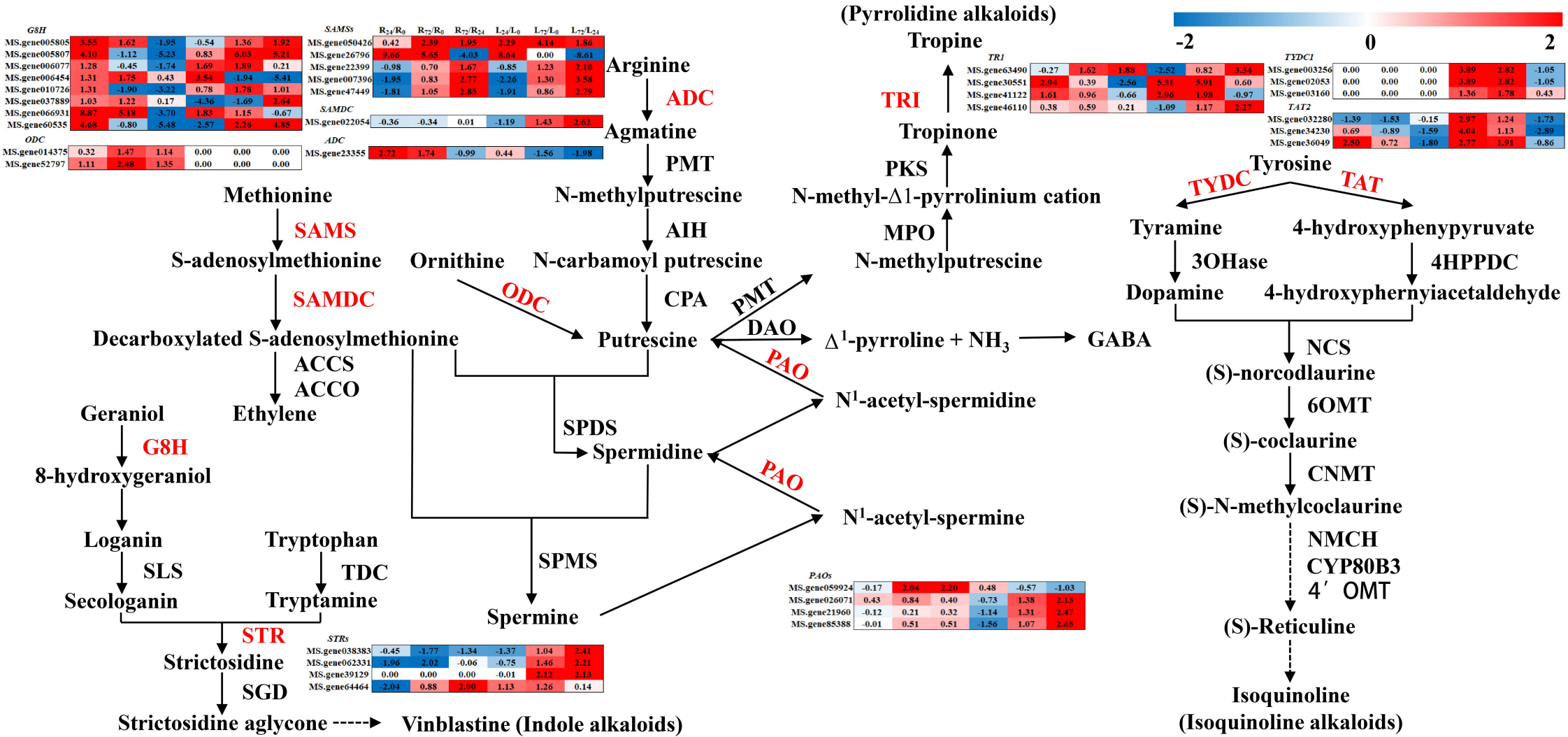

A
Number of DEGs
12000
10000
8000
6000
4000
2000
0
Upregulated
Downregulated
8341
8116
6299
8228
7286
9681
8075
10135
5612
7275
7636
7202
R24/R0
R72/R0
R72/R24
L24/L0
L72/L0
L72/L24
B
R72/R0
L24/L0
3101
4308
86
1352
1361
4512
220
232
2184
379
1111
689
R24/R0
378
240
L72/L0
149
C
R72/R0
L24/L0
3423
4881
187
1928
2274
3377
313
443
2166
667
1029
923
R24/R0
341
344
L72/L0
117


A
GO enrichment analysis(R24/R0)
Oxidoreductase activity
Heme binding
Tetrapyrrole binding
Extracellular region
Membrane
Oxidoreductase activity, acting on paired donors
Secondary metabolic process
Plasma membrane
Monooxygenase activity
Small molecule metabolic process
Iron ion binding
Phenylpropanoid metabolic process
Antioxidant activity
Lactoperoxidase activity
Catalytic activity
Transmembrane transporter activity
Transporter activity
Lignin metabolic process
Lignin catabolic process
Phenylpropanoid catabolic process
GO term
Rich factor
0.05 0.1 0.15 0.2 0.25 0.3 0.35 0.4 0.45 0.5 0.55 0.6
Padjust
3.00e-25
2.50e-25
2.00e-25
1.50e-25
1.00e-25
5.00e-26
0.00e+0
Number
53
2768
5482
8279
B
GO enrichment analysis(R72/R0)
Oxidoreductase activity
Heme binding
Tetrapyrrole binding
Secondary metabolic process
Phenylpropanoid metabolic process
Structural molecule activity
Olefinic compound metabolic process
Ribosomal subunit
Cellular amide metabolic process
Secondary metabolite biosynthetic process
Peptide metabolic process
Cytosolic large ribosomal subunit
Structural constituent of ribosome
Plasma membrane
Olefinic compound biosynthetic process
Translation
Oxidoreductase activity, acting on paired donors
Peptide biosynthetic process
Large ribosomal subunit
Small molecule metabolic process
GO term
Rich factor
0.05 0.1 0.15 0.2 0.25 0.3 0.35 0.4 0.45
Padjust
1.40e-15
1.20e-15
1.00e-15
8.00e-16
6.00e-16
4.00e-16
2.00e-16
0.00e+0
Number
44
464
884
1317
C
GO enrichment analysis(R72/R24)
Oxidoreductase activity
Heme binding
Tetrapyrrole binding
Secondary metabolic process
Phenylpropanoid metabolic process
Catalytic activity
Oxidoreductase activity, acting on paired donors
Membrane
Extracellular region
Monooxygenase activity
Iron ion binding
Small molecule metabolic process
Lignin catabolic process
Phenylpropanoid catabolic process
Plasma membrane
Carbohydrate metabolic process
Lignin metabolic process
Apoplast
Hydroquinone:oxygen oxidoreductase activity
Protein kinase activity
GO term
Rich factor
0.05 0.1 0.15 0.2 0.25 0.3 0.35 0.4 0.45 0.5 0.55 0.6 0.65
Padjust
2.00e-27
1.50e-27
1.00e-27
5.00e-28
0.00e+0
Number
59
2942
5824
8794
D
GO enrichment analysis(L24/L0)
Oxidoreductase activity
Small molecule metabolic process
Carbohydrate metabolic process
Plastid
Cellular carbohydrate metabolic process
Carboxylic acid metabolic process
Chloroplast
Organic acid metabolic process
Catalytic activity
Oxoacid metabolic process
Membrane
Organic substance biosynthetic process
Biosynthetic process
Organonitrogen compound biosynthetic process
Phosphoric ester hydrolase activity
Cellular amino acid metabolic process
Small molecule biosynthetic process
Lipid metabolic process
Small molecule binding
Cellular polysaccharide metabolic process
GO term
Rich factor
0.1 0.11 0.12 0.13 0.14 0.15 0.16 0.17 0.18 0.19 0.2 0.21
Padjust
8.00e-17
6.00e-17
4.00e-17
2.00e-17
0.00e+0
Number
259
3188
6118
9136
E
GO enrichment analysis(L72/L0)
Tertiary alcohol metabolic process
Abscisic acid metabolic process
Apocarotenoid metabolic process
Cinnamic acid biosynthetic process
Cinnamic acid metabolic process
Sesquiterpenoid metabolic process
Regulation of salicylic acid metabolic process
Regulation of jasmonic acid mediated signaling pathway
Tertiary alcohol biosynthetic process
Abscisic acid biosynthetic process
Apocarotenoid biosynthetic process
Glucosamine-containing compound catabolic process
Chitin metabolic process
Amino sugar catabolic process
Aminoglycan catabolic process
Chitin catabolic process
Box C/D RNP complex
12-oxophytodienoate reductase activity
(+)-abscisic acid 8'-hydroxylase activity
Photosynthesis, light harvesting in photosystem I
GO term
Rich factor
0.2 0.25 0.3 0.35 0.4 0.45 0.5 0.55
Padjust
2.50e-4
2.40e-4
2.30e-4
2.20e-4
2.10e-4
2.00e-4
1.90e-4
Number
13
21
28
36
F
GO enrichment analysis(L72/L24)
Structural constituent of ribosome
Ribosomal subunit
Translation
Amide biosynthetic process
Peptide biosynthetic process
Organonitrogen compound biosynthetic process
Peptide metabolic process
Cellular amide metabolic process
Cellular macromolecule biosynthetic process
Structural molecule activity
Organic substance biosynthetic process
Biosynthetic process
Ribosome
Oxidoreductase activity
Large ribosomal subunit
Cytosolic large ribosomal subunit
Cellular biosynthetic process
Ribonucleoprotein complex
Small molecule metabolic process
Small ribosomal subunit
GO term
Rich factor
0.1 0.12 0.14 0.16 0.18 0.2 0.22 0.24 0.26 0.28 0.3
Padjust
4.00e-29
3.00e-29
2.00e-29
1.00e-29
0.00e+0
Number
139
675
1210
1762

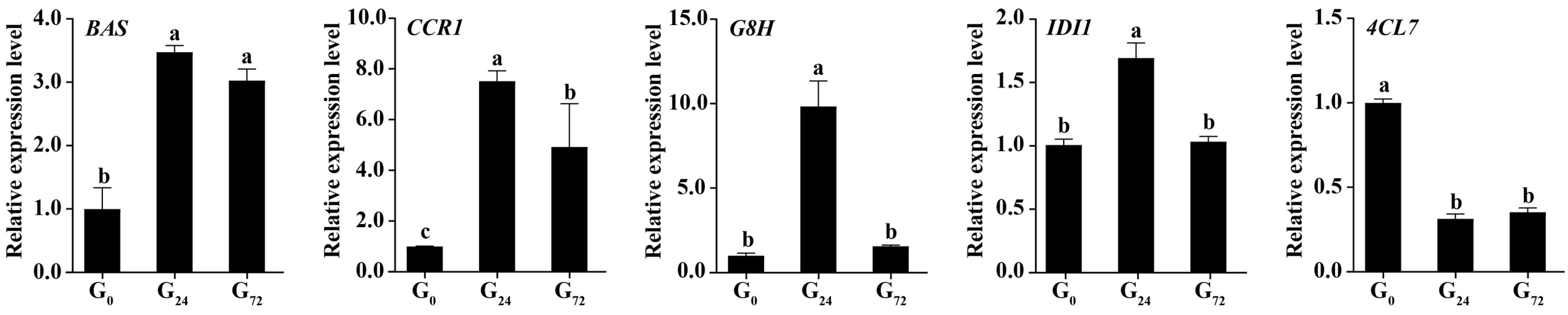

A
KEGG enrichment analysis(R_{24}/R_0)
Phenylpropanoid biosynthesis
Nitrogen metabolism
Biosynthesis of various plant secondary metabolites
MAPK signaling pathway-plant
Glutathione metabolism
Starch and sucrose metabolism
Linoleic acid metabolism
ABC transporters
Cysteine and methionine metabolism
Glucosinolate biosynthesis
Amino sugar and nucleotide sugar metabolism
Cutin, suberine and wax biosynthesis
Valine, leucine and isoleucine degradation
Riboflavin metabolism
Cyanoamino acid metabolism
Tropane, piperidine and pyridine alkaloid biosynthesis
Aflatoxin biosynthesis
Stilbenoid, diarylheptanoid and gingerol biosynthesis
Peroxisome
Alanine, aspartate and glutamate metabolism
KEGG pathway
0.1 0.15 0.2 0.25 0.3 0.35 0.4 0.45 0.5 0.55
Rich Factor
Padjust
0.00800
0.00600
0.00400
0.00200
0.00
Number
6
77
148
221
B
KEGG enrichment analysis(R_{72}/R_0)
Phenylpropanoid biosynthesis
Ribosome
Circadian rhythm - plant
Tropane, piperidine and pyridine alkaloid biosynthesis
Isoflavonoid biosynthesis
Biosynthesis of various plant secondary metabolites
MAPK signaling pathway-plant
Starch and sucrose metabolism
Flavonoid biosynthesis
Nitrogen metabolism
Cyanoamino acid metabolism
Linoleic acid metabolism
Galactose metabolism
Cutin, suberine and wax biosynthesis
Monoterpenoid biosynthesis
Pyrimidine metabolism
Alanine, aspartate and glutamate metabolism
Amino sugar and nucleotide sugar metabolism
Diterpenoid biosynthesis
Plant-pathogen interaction
KEGG pathway
0.1 0.12 0.14 0.16 0.18 0.2 0.22 0.24 0.26
Rich Factor
Padjust
0.200
0.150
0.100
0.0500
0.00
Number
17
100
183
268
C
KEGG enrichment analysis(R_{72}/R_{24})
Phenylpropanoid biosynthesis
Isoflavonoid biosynthesis
Biosynthesis of various plant secondary metabolites
Nitrogen metabolism
MAPK signaling pathway-plant
Glutathione metabolism
Galactose metabolism
Tropane, piperidine and pyridine alkaloid biosynthesis
Cysteine and methionine metabolism
Flavonoid biosynthesis
Cyanoamino acid metabolism
Amino sugar and nucleotide sugar metabolism
ABC transporters
Glucosinolate biosynthesis
Starch and sucrose metabolism
Circadian rhythm-plant
Ribosome
Linoleic acid metabolism
Cutin, suberine and wax biosynthesis
Phenylalanine metabolism
KEGG pathway
0.1 0.15 0.2 0.25 0.3 0.35 0.4 0.45
Rich Factor
Padjust
0.000350
0.000300
0.000250
0.000200
0.000150
0.000100
0.0000500
0.00
Number
17
95
173
253
D
KEGG enrichment analysis(L_{24}/L_0)
Porphyrin metabolism
Isoquinoline alkaloid biosynthesis
alpha-Linolenic acid metabolism
Tyrosine metabolism
Photosynthesis - antenna proteins
Carbon fixation in photosynthetic organisms
Carotenoid biosynthesis
Phenylalanine metabolism
Tropane, piperidine and pyridine alkaloid biosynthesis
Photosynthesis
Riboflavin metabolism
Cysteine and methionine metabolism
Glutathione metabolism
Starch and sucrose metabolism
Glyoxylate and dicarboxylate metabolism
Arginine and proline metabolism
MAPK signaling pathway-plant
Amino sugar and nucleotide sugar metabolism
Glycolysis / Gluconeogenesis
Nitrogen metabolism
KEGG pathway
0.16 0.18 0.2 0.22 0.24 0.26 0.28 0.3 0.32 0.34 0.36 0.38
Rich Factor
Padjust
0.00100
0.000800
0.000600
0.000400
0.000200
0.00
Number
29
78
127
178
E
KEGG enrichment analysis(L_{72}/L_0)
Ribosome
MAPK signaling pathway-plant
Riboflavin metabolism
Plant-pathogen interaction
Amino sugar and nucleotide sugar metabolism
Glutathione metabolism
Photosynthesis - antenna proteins
Carotenoid biosynthesis
alpha-Linolenic acid metabolism
Starch and sucrose metabolism
Carbon fixation in photosynthetic organisms
Glucosinolate biosynthesis
Phenylpropanoid biosynthesis
Ribosome biogenesis in eukaryotes
Pentose phosphate pathway
Biosynthesis of nucleotide sugars
Terpenoid backbone biosynthesis
Photosynthesis
Tropane, piperidine and pyridine alkaloid biosynthesis
Circadian rhythm-plant
KEGG pathway
0.1 0.12 0.14 0.16 0.18 0.2 0.22 0.24 0.26 0.28 0.3
Rich Factor
Padjust
0.0300
0.0250
0.0200
0.0150
0.0100
0.00500
0.00
Number
11
87
162
240
F
KEGG enrichment analysis(L_{72}/L_{24})
Ribosome
Porphyrin metabolism
Selenocompound metabolism
Tropane, piperidine and pyridine alkaloid biosynthesis
MAPK signaling pathway-plant
Arginine and proline metabolism
Aflatoxin biosynthesis
Glutathione metabolism
Circadian rhythm-plant
Amino sugar and nucleotide sugar metabolism
Ascorbate and aldarate metabolism
Tyrosine metabolism
Plant hormone signal transduction
Fatty acid biosynthesis
Purine metabolism
Galactose metabolism
Isoquinoline alkaloid biosynthesis
Cysteine and methionine metabolism
Sulfur metabolism
Glyoxylate and dicarboxylate metabolism
KEGG pathway
0.05 0.1 0.15 0.2 0.25 0.3 0.35 0.4 0.45 0.5 0.55 0.6 0.65
Rich Factor
Padjust
0.0150
0.0100
0.00500
0.00
Number
7
146
284
427


-2
0
2
Tyrosine
PAL
Cinnamic acid
PAL
Phenylalanine
C4H
Coumaric acid
4CL
P-coumaroyl CoA
CHS
Naringenin chalcone
CHI
Flavanone
CHI
Naringenin
FNS
Flavone
IFS
Isoflavone
F3H
Dihydrokaempferol
F3′H
Dihydroquercetin
DFR
Leucocyanidin
ANS
Cyanidin
UFGT
Anthocyanin
F3H
Dihydroflavonol
FLS
Flavanol
ANR
Epicatechin
LAR
Flavanol
FLS
Quercetin
F3′H
Kaempferol
FLS
Isorhamnetin
HCT
P-coumaroyl shikimate
C3′H
Caffeoyl shikimate
CSE
Caffeic acid
COMT
Ferulic acid
F5H
5-hydroxyferulic acid
COMT
Sinapic acid
HCT
Caffeoyl CoA
CCoAOMT
Feruloyl-CoA
CCR
Caffealdehyde
COMT
Coniferaldehyde
F5H
5-hydroxyconifer-aldehyde
COMT
Sinapaldehyde
CAD
Caffeylalcohol
COMT
Coniferylalcohol
F5H
5-hydroxyconiferyl aldehyde
COMT
Sinapylalcohol
CAD
CAD
CAD
4CLL9
R24/R0 R72/R0 R72/R24 L24/L0 L72/L0 L72/L24
MS.gene022445 1.32 1.07 -0.26 -0.76 -1.65 -0.87
MS.gene004713 1.60 -0.19 -1.80 2.45 1.35 -1.09
HCT
MS.gene054539 -0.44 -0.25 0.18 -0.69 1.46 2.16
CSE
MS.gene75172 0.00 6.65 6.67 0.00 4.59 4.73
MS.gene76310 1.28 1.51 0.22 -1.08 0.83 1.94
CCR1
MS.gene64416 0.15 1.43 1.26 5.18 3.34 -1.80
MS.gene034132 -0.57 0.76 1.31 1.27 1.27 0.01
MS.gene052599 1.00 -0.64 -1.66 1.19 1.53 0.36
COMT1
MS.gene024383 0.02 1.11 1.08 0.87 1.38 0.53
MS.gene020301 -0.36 0.19 0.54 1.10 1.23 0.14
MS.gene065217 0.79 -1.05 -1.85 -1.11 1.65 2.75
MS.gene069457 1.45 -0.46 -1.92 1.33 2.01 0.69
CADs
MS.gene002258 1.43 2.29 0.85 -0.17 -0.52 -0.33
MS.gene002257 -1.82 -2.39 -0.59 2.81 2.29 -0.50
MS.gene01231 -1.16 0.73 1.88 -0.73 3.30 4.03
MS.gene02214 0.86 0.70 -0.17 1.35 1.06 -0.28
MS.gene065692 2.11 -0.04 -2.16 3.16 1.56 -1.59
ANR
MS.gene01410 0.49 0.78 0.28 -0.01 1.78 1.79
UFGT7
MS.gene00212 0.34 1.45 1.09 -0.20 -0.10 0.11
MS.gene011829 -0.84 1.30 2.13 1.91 0.11 2.03
MS.gene28593 0.21 1.49 1.27 0.00 0.00 0.00
MS.gene049907 3.32 1.56 -1.77 -0.84 0.53 1.38
MS.gene67515 0.15 2.15 1.99 -2.39 0.62 3.02
MS.gene90522 -0.64 1.28 1.91 0.00 0.00 0.00
MS.gene99188 0.00 4.76 4.79 0.00 0.00 0.00
MS.gene036571 1.63 -0.20 -1.84 2.77 2.06 -0.70
MS.gene21268 5.88 3.10 -2.79 0.65 1.80 1.17
CCoAOMTs
MS.gene011778 -0.34 -0.17 0.15 3.06 2.20 -0.85
MS.gene030303 3.21 2.25 -0.97 0.23 1.72 1.51
MS.gene041940 -0.34 -0.17 0.15 3.06 2.20 -0.85
MS.gene56793 -0.06 1.33 1.38 -0.34 0.28 0.62
MS.gene90469 -0.34 -0.17 0.15 3.06 2.20 -0.85
MS.gene99216 0.17 1.22 1.04 0.88 0.71 -0.16

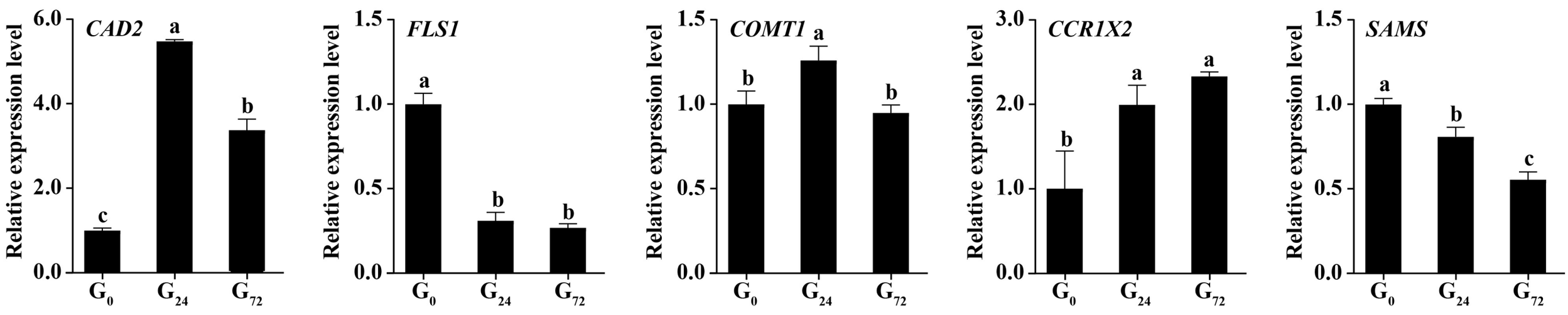

MVA pathway
MEP pathway
-2
0
2
Acetyl-CoA
AACT
Acetoacetyl-CoA
HMGS
3-hydroxy-3-methyl-glutaryl Co A
HMGR
Mevalonic acid
MVK
Phosphomevalonate
PMK
Diphosphomevalonate
MVD
Dimethylallyl diphosphate
IDI
Isopentenyl pyrophosphate
FDS
FDS
Other sesquiterpenes
Farnesyl diphosphate
GAS
ECS
CPS
BFS
SQS
Germacrene A
8-epi-cedrol
Squalene
β-farnesene
β-caryophyllene
BAS
SQE
SMO
Triterpene
2,3-oxido-squalene
BAS
β-amyrin
Sterols
Other triterpenes
Glyceraldehyde 3-phosphate + Pyruvic acid
DXS
1-deoxy-D-xylulose 5-phosphate
DXR
2-C-methyl-D-erythritol-4-phosphate
MCT
4-cytidine 5′-diphospho-2-C-methyl-D-erythritol
CMK
2-phospho-4-cytidine 5′-diphospho-2-C-methyl-D-erythritol
MCS
2-C-methyl-D-erythritol-2,4-cyclodiphosphate
HDS
Hydroxy-2-methyl-2-(E)-butenyl 4-diphosphate
HDR
HDR
IDI
Isopentenyl pyrophosphate
Dimethylallyl diphosphate
GDS
GDS
Geranyl diphosphate
Other monoterpenes
LS
GGDS
BPS
Linalool
Geranylgeranyl diphosphate
β-pinene
Diterpenes
Plastoquinones
Chlorophyls
Carotenoids
Gibberelins
Tocopherols
HMGS
R24/R0 R72/R0 R72/R24 L24/L0 L72/L0 L72/L24
MS.gene015517 6.27 6.81 0.52 0.00 4.57 4.70
MS.gene025733 0.38 3.27 2.88 0.75 1.18 0.44
MVK
MS.gene072461 -0.20 1.08 1.26 -0.41 -1.53 -1.11
IDIs
MS.gene033475 1.33 1.71 0.37 1.47 1.76 0.31
MS.gene51160 0.19 1.95 1.75 0.39 1.69 1.32
BAS
MS.gene034307 1.08 1.58 0.49 -0.24 0.15 0.40
MS.gene019797 -0.43 1.07 1.49 2.32 0.98 -1.33
SQS2
MS.gene50719 2.38 2.02 -0.38 1.29 0.99 -0.29
GGDS
MS.gene87404 -1.84 -0.08 1.74 -0.03 1.13 1.18
MS.gene28490 -1.81 -0.58 1.23 8.72 2.28 11.00
SMOs
MS.gene80337 0.04 2.54 2.47 0.00 0.00 0.00
MS.gene32851 -1.18 0.30 1.47 -0.27 1.03 1.31
SQE1
MS.gene24516 1.09 1.91 0.81 -1.95 -0.24 1.72
MS.gene40110 0.52 1.75 1.22 -0.30 0.82 1.13
MS.gene001138 -0.63 -1.14 -0.52 -0.06 1.68 1.77
DXS
MS.gene014804 1.11 0.71 -0.41 1.42 1.17 -0.24
MS.gene060356 1.08 0.95 -0.15 1.58 1.52 -0.05
MS.gene96182 6.47 5.40 -1.08 0.00 0.00 0.00
HDR
MS.gene40678 0.21 1.35 1.12 0.11 1.20 1.10

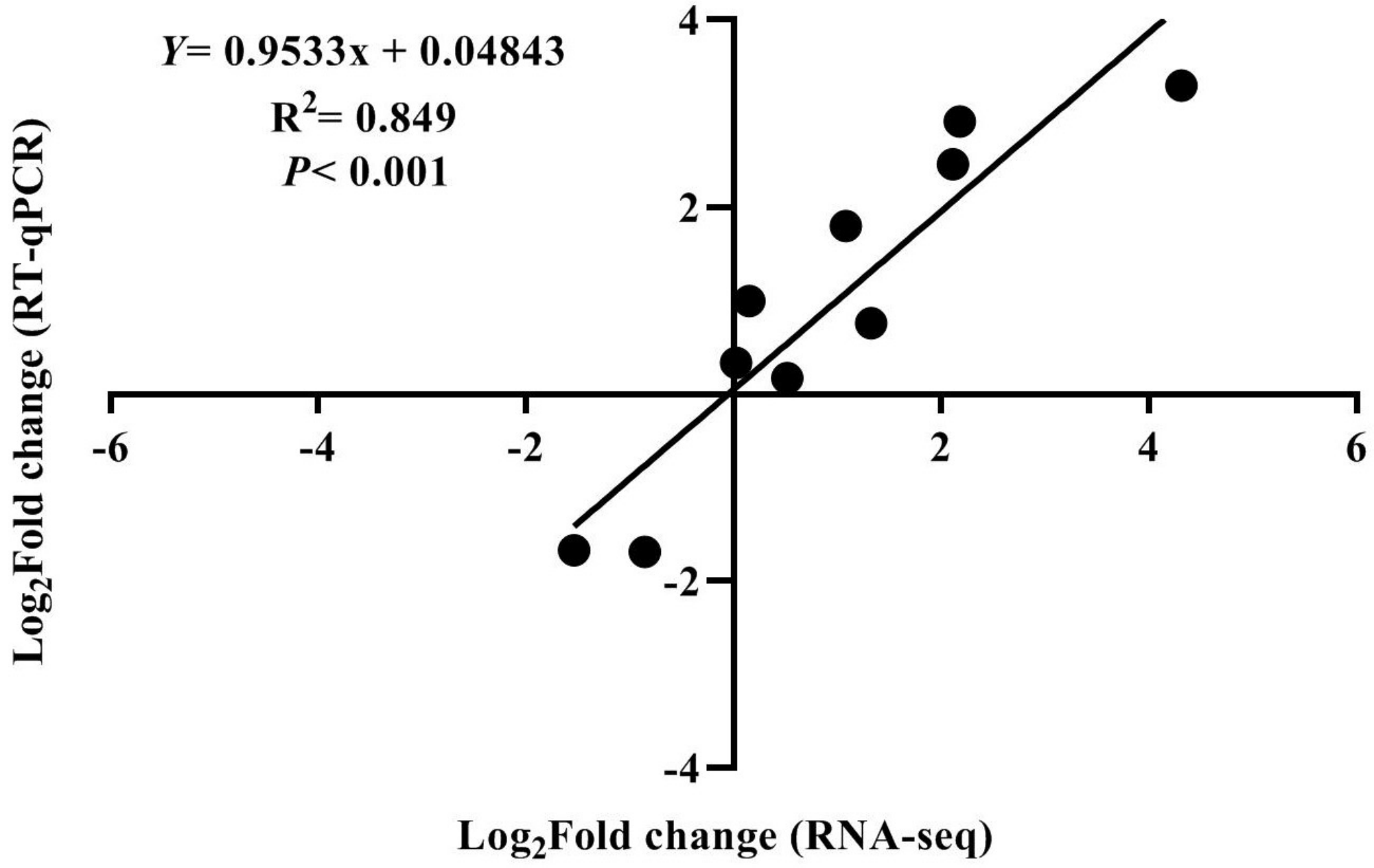

G8H
MS.gene005805 3.55 1.62 -1.95 -0.54 1.36 1.92
MS.gene005807 4.10 -1.12 -5.23 0.83 6.03 5.21
MS.gene006077 1.28 -0.45 -1.74 1.69 1.89 0.21
MS.gene006454 1.31 1.75 0.43 3.54 -1.94 -5.41
MS.gene010726 1.31 -1.90 -3.22 0.78 1.78 1.01
MS.gene037889 1.03 1.22 0.17 -4.36 -1.69 2.64
MS.gene066931 8.87 5.18 -3.70 1.83 1.15 -0.67
MS.gene60535 4.68 -0.80 5.48 -2.57 2.26 4.85
ODC
MS.gene014375 0.32 1.47 1.14 0.00 0.00 0.00
MS.gene52797 1.11 2.48 1.35 0.00 0.00 0.00
SAMSs
R24/R0 R72/R0 R72/R24 L24/L0 L72/L0 L72/L24
MS.gene050426 0.42 2.39 1.95 2.29 4.14 1.86
MS.gene26796 9.66 5.65 -4.03 8.64 0.00 -8.61
MS.gene22399 -0.98 0.70 1.67 -0.85 1.23 2.10
MS.gene007396 -1.95 0.83 2.77 -2.26 1.30 3.58
MS.gene47449 -1.81 1.05 2.85 -1.91 0.86 2.79
SAMDC
MS.gene022054 -0.36 -0.34 0.01 -1.19 1.43 2.62
ADC
MS.gene23355 2.72 1.74 -0.99 0.44 -1.56 -1.98
(Pyrrolidine alkaloids)
Tropine
TRI
Tropinone
PKS
N-methyl-Δ1-pyrrolinium cation
MPO
N-methylputrescine
TRI
MS.gene63490 -0.27 1.62 1.88 -2.52 0.82 3.34
MS.gene30551 2.94 0.39 -2.56 5.31 5.91 0.60
MS.gene41122 1.61 0.96 -0.66 2.96 1.98 -0.97
MS.gene46110 0.38 0.59 0.21 -1.09 1.17 2.27
-2
0
2
TYDC1
MS.gene003256 0.00 0.00 0.00 3.89 2.82 -1.05
MS.gene02053 0.00 0.00 0.00 3.89 2.82 -1.05
MS.gene03160 0.00 0.00 0.00 1.36 1.78 0.43
TAT2
MS.gene032280 -1.39 -1.53 -0.15 2.97 1.24 -1.73
MS.gene34230 0.69 -0.89 -1.59 4.04 1.13 -2.89
MS.gene36049 2.50 0.72 -1.80 2.77 1.91 -0.86
Arginine
ADC
Agmatine
PMT
N-methylputrescine
AIH
Methionine
SAMS
S-adenosylmethionine
Ornithine
N-carbamoyl putrescine
SAMDC
ODC
CPA
PMT
DAO
PAO
Decarboxylated S-adenosylmethionine
Putrescine
Δ1-pyrroline + NH3
GABA
ACCS
ACCO
Ethylene
SPDS
N1-acetyl-spermidine
Geraniol
G8H
8-hydroxygeraniol
Spermidine
PAO
Loganin
SLS
Secologanin
Tryptophan
TDC
Tryptamine
SPMS
N1-acetyl-spermine
Spermine
PAOs
MS.gene059924 -0.17 2.04 2.20 0.48 -0.57 -1.03
MS.gene026071 0.43 0.84 0.40 -0.73 1.38 2.13
MS.gene21960 -0.12 0.21 0.32 -1.14 1.31 2.47
MS.gene85388 -0.01 0.51 0.51 -1.56 1.07 2.65
STR
Strictosidine
SGD
STRs
MS.gene038383 -0.45 -1.77 -1.34 -1.37 1.04 2.41
MS.gene062331 -1.96 -2.02 -0.06 -0.75 1.46 2.21
MS.gene39129 0.00 0.00 0.00 -0.01 2.12 2.13
MS.gene64464 -2.04 0.88 2.90 1.13 1.26 0.14
Strictosidine aglycone
Vinblastine (Indole alkaloids)
Tyrosine
TYDC
TAT
Tyramine
4-hydroxyphenypyruvate
3OHase
4HPPDC
Dopamine
4-hydroxyphernyiacetaldehyde
NCS
(S)-norcodlaurine
6OMT
(S)-coclaurine
CNMT
(S)-N-methylcoclaurine
NMCH
CYP80B3
4′ OMT
(S)-Reticuline
Isoquinoline
(Isoquinoline alkaloids)

A


BAS
CCR1
G8H
IDI1
4CL7
CAD2
FLS1
COMT1
CCR1X2
SAMS
Relative expression level
G0
G24
G72

B


BAS
CCR1
G8H
IDI1
4CL7
CAD2
FLS1
COMT1
CCR1X2
SAMS
Relative expression level
G0
G24
G72


Y= 0.9533x + 0.04843
R2= 0.849
P< 0.001
4
2
-2
-4
-6
-4
-2
2
4
6
Log2Fold change (RT-qPCR)
Log2Fold change (RNA-seq)

Supplementary Files

This is a list of supplementary files associated with this preprint. Click to download.

- SupportingInformation.xlsx